

**Fig. 3.62**  $^1\text{H}$  NMR spectrum of **44** (aliphatic portion); **a** measured, **b** simulated AA'BB' system (Meier, H., Gugel, H., Kolschorn, H. (1976), *Z. Naturforsch., Part B*, **31**, 1270)

### NMR Spectra of Oriented Phases and Solids

Certain compounds form liquid crystalline states (nematic, smectic, or cholesteric) between the melting point and the clarification point; in these phases the molecules have a pre-

ferred orientation. Apart from the **thermotropic liquid crystalline phases** there are **lyotropic liquid crystalline phases**, which can be formed by amphiphilic compounds, e.g. tensides, and water or other solvents.

Nematic phases are often composed of linear molecules, which are orientated in a specific direction. Guest molecules introduced into the phase then have their Brownian motion restricted and are forced into a similar preferred orientation. In the NMR spectra this preferred orientation is apparent from the direct dipolar couplings between the nuclear spins of the guest molecule; the result is additional splittings of the lines. Partially oriented molecules consequently give multiline spectra, several kHz broad, since the dipolar couplings are much larger than the coupling constants which result from scalar interactions. The analysis of such spectra can yield valuable information about structural parameters such as bond angles and bond lengths, which are related to the geometry of the molecules in liquid phase.

On going from partially oriented phases to the solid phase, the number of spin-spin interactions is drastically increased, because now the **intermolecular** interactions also come into play; for guest molecules in oriented liquid crystalline phases these are eliminated by the translational and rotational motions. The signals therefore become very broad in solids. In Sec. 4.8 (see p. 180 ff.) the use of **magic-angle spinning** to obtain high resolution spectra from solids is described.

Finally it should be mentioned that NMR can be used not only for observations on individual molecules or aggregates of molecules, but that methods such as NMR imaging and nuclear spin tomography have been developed which can provide pictures of macroscopic objects. For biology and above all for medicinal purposes these methods have become immensely important, allowing images (cross sections) of internal organs to be acquired without physical intervention or the use of dangerous radiation.

## 4. $^{13}\text{C}$ NMR Spectroscopy

### 4.1 Sample Preparation and Measurement of Spectra

For the measurement of a  $^{13}\text{C}$  spectrum the sample needs to be fairly concentrated, but not viscous. As a rule of thumb, a fast routine measurement requires 3 mg of sample (dissolved in 0.6 ml of solution) for each carbon atom in the molecules. The PFT method is used (see Sec. 3.1, p. 100).

The usual **solvent** is deuteriochloroform. A summary of alternative solvents is given in Tab. 3.24. Deuteriated solvents are

used to facilitate the measurement by employment of the deuterium resonance of the solvent as a **lock signal** to stabilise the field-frequency relationship in the spectrometer. A further advantage of deuteriated solvents is that their  $^{13}\text{C}$  signals are weaker than those of protonated solvents, as a combined result of the splitting of the  $^{13}\text{C}$  signal by deuterium (see Tab. 3.24), the lack of the NOE enhancement (see p. 85), and the longer relaxation times  $T_1$ . The relatively strong  $^{13}\text{C}$  signals of protonated solvents or of deuteriated solvents in dilute solutions can lead to problems of dynamic range (ability to

Solvents for <sup>13</sup>C NMR spectroscopy

Solvent	<sup>13</sup> C NMR shift δ	Multiplicity	J( <sup>13</sup> C,D) (Hz)	
[D <sub>2</sub> ] Chloroform	77.0	triplet	32	
[D <sub>2</sub> ] Methanol	49.3	septet	21	T
[D <sub>2</sub> ] Acetone	29.3	septet	20	T
	206.3	multiplet	<1	
[D <sub>6</sub> ] Benzene	128.0	triplet	24	
[D <sub>2</sub> ] Dichloromethane	53.5	quintet	27	T
[D <sub>3</sub> ] Acetonitrile	1.3	septet	21	
	117.7	multiplet	<1	
[D <sub>2</sub> ] Bromoform	10.2	triplet	31.5	H
[D <sub>2</sub> ] 1,1,2,3-Tetrachloroethane	74.0	triplet		
[D <sub>4</sub> ] Tetrahydrofuran	25.5	quintet	21	
	67.7	quintet	22	
[D <sub>6</sub> ] Dioxane	66.5	quintet	22	
[D <sub>2</sub> ] Dimethyl sulfoxide	39.7	septet	21	
[D <sub>3</sub> ] Pyridine	123.5	triplet	25	
	135.5	triplet	24	
	149.5	triplet	27	
[D <sub>2</sub> ] Water	-	-	-	
[D <sub>2</sub> ] Acetic acid	20.0	septet	20	
	178.4	multiplet	<1	
[D <sub>10</sub> ] Hexamethylphosphoric triamide (HMPT)	35.8	septet	21	H
Carbon tetrachloride	96.0	singlet	-	
Carbon disulfide	192.8	singlet	-	T
Trichlorofluoromethane	117.6	doublet	( <sup>1</sup> J(C,F)=337)	T
[D <sub>2</sub> ] Trifluoroacetic acid	116.5	quartet	( <sup>1</sup> J(C,F)=283)	
	164.4	quartet	( <sup>2</sup> J(C,F)=44)	

T suitable for low temperature measurements (see Tab. 3.6)  
 H suitable for high temperature measurements (see Tab. 3.6)

As in <sup>1</sup>H NMR tetramethylsilane (TMS) may be used as a **reference** to establish the zero point of the δ scale (internal or external standard). Frequently the <sup>13</sup>C signals of the solvent with their known shifts suffice for the determination of the δ values of the sample.

The low natural <sup>13</sup>C content of 1.1% and the low magnetic moment mean that the <sup>13</sup>C nucleus has a low NMR sensitivity (see Sec. 1.1, especially Tab. 3.1, p. 72).

In measurements of <sup>13</sup>C spectra of organic compounds there *will normally be hydrogen nuclei present in the molecule*, which give rise to spin-spin couplings; that means that for a set of isochronous <sup>13</sup>C nuclei a multiplet will be expected, caused by direct, *geminal*, and *vicinal* couplings. The signal intensity will thereby be distributed over several lines. In <sup>1</sup>H NMR these <sup>13</sup>C,<sup>1</sup>H couplings are normally not apparent because of the low natural abundance of <sup>13</sup>C (see however Sec. 3.9, p. 129 on <sup>13</sup>C satellites). This problem is generally avoided in <sup>13</sup>C NMR by using **<sup>1</sup>H broadband decoupling**. In contrast to **homonuclear spin decoupling** (Sec. 3.8, p. 131) this is a **heteronuclear spin decoupling** technique.

In order to simultaneously remove all the <sup>13</sup>C,<sup>1</sup>H couplings present, a powerful irradiation is used which covers the whole proton chemical shift range. The decoupler frequency is modulated with low frequency noise. This has led to the use of the term **<sup>1</sup>H noise decoupling** as an alternative to **<sup>1</sup>H broadband decoupling**. Even more effective methods of decoupling using phase modulation are now replacing noise modulation (Waugh, GARP, etc.).

The decoupling effect, as described on p. 131 ff, depends on the coupling <sup>1</sup>H nuclei changing their precession direction (spin orientation) so rapidly as a result of the irradiation at their resonance frequency that all their coupling partners (here the coupling <sup>13</sup>C nuclei) only experience an average value of zero. All the lines of the multiplet of a <sup>13</sup>C signal form a singlet as a result. Its intensity can amount to 300% of the intensity of the individual lines of the multiplet. Part of this increased intensity is a consequence of the **heteronuclear Overhauser effect** (see Sec. 1.5, p. 84).

observe weak signals in the presence of strong ones) in the computer or can obscure weak signals of the sample. The first problem is largely avoided in modern spectrometers by the use of 32 bit technology (older spectrometers often use 24 or 16 bits) and the second can be avoided by the use of commercially available solvents which are depleted in <sup>13</sup>C. In these the natural <sup>13</sup>C content of 1.1% is reduced to ca. 0.1%. (Additionally there are instrumental techniques available to reduce the intensity of solvent signals: pre-saturation, Redfield technique, etc.)



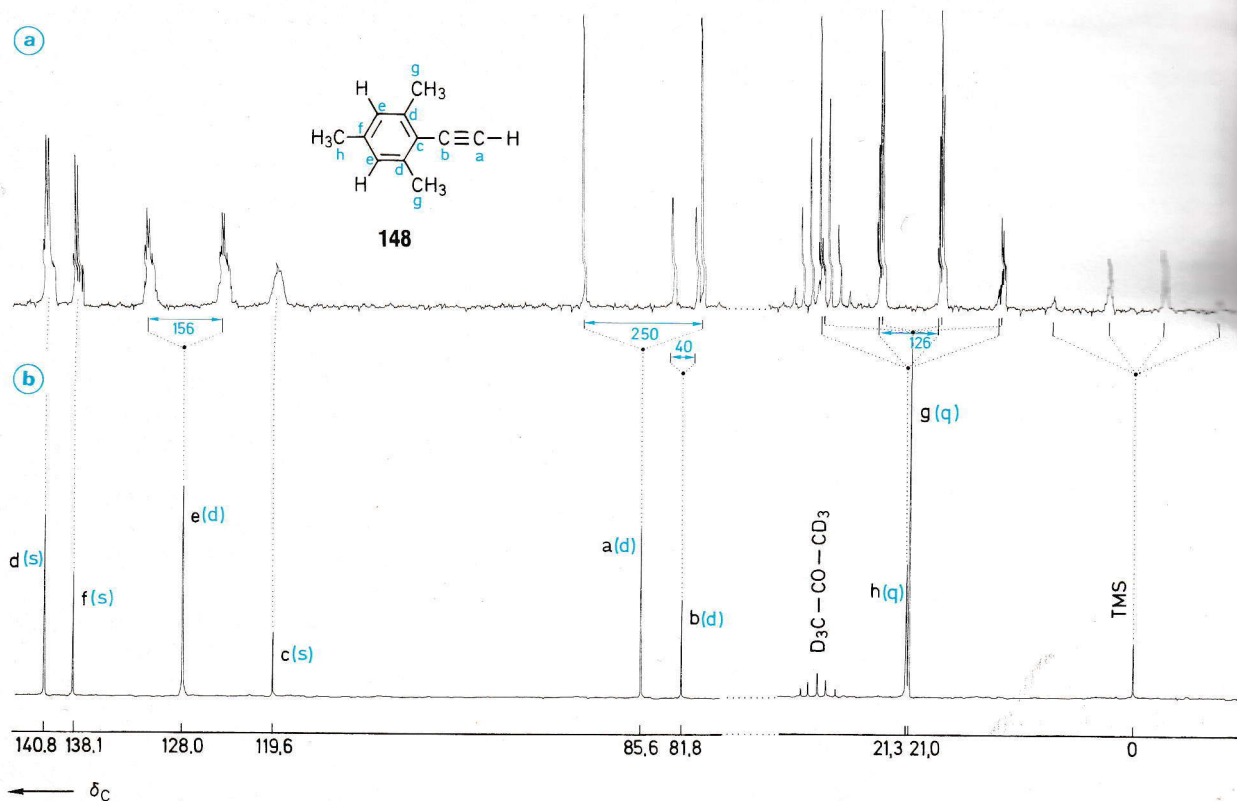


**Fig. 3.63**  $^{13}\text{C}$  NMR spectra of mesitylacetylene (**148**) in hexadeuterioacetone **a** coupled **b**  $^1\text{H}$  broadband decoupled

The  $^1\text{H}$  broadband decoupling simplifies the  $^{13}\text{C}$  NMR spectra considerably, and the signals gain in intensity. These advantages outweigh the loss of information from  $^{13}\text{C}$ ,  $^1\text{H}$  coupling so much that routine  $^{13}\text{C}$  spectra are always acquired with broadband decoupling. The  $^{13}\text{C}$ , D couplings remain unaffected. Fig. 3.63 shows as an example a comparison of coupled and  $^1\text{H}$  broadband decoupled  $^{13}\text{C}$  spectra for mesitylacetylene (**141**).

In the decoupled spectrum 3.63b the signals d, f, and c remain in the same positions as in 3.63a. They are singlets (s). The corresponding C atoms are not bonded to hydrogen. In the coupled spectrum 3.63a their signals are only broadened by couplings to more distant protons. The signals e, a, and b each appear in the coupled spectrum as a doublet (d), i.e. the corresponding C nuclei couple, apart from long range couplings, to only one proton. The three coupling constants, 156, 250, and 40 Hz, differ widely. For e and a the coupling is to a directly bonded proton ( $^1J(\text{C},\text{H})$ ) for an aromatic carbon and an acetylenic carbon respectively. For b an unusually large  $^2J(\text{C},\text{H})$  is observed (see Sec. 4.3, p. 149). The methyl C nuclei g and h each show a quartet (q) from coupling to the three methyl protons. Only in the decoupled spectrum is it easily apparent that

there are two signals, with such different intensities that the higher peak can be assigned to the two carbon atoms g. (A  $\text{CH}_2$  group would give a triplet (t), but there is none in this molecule.)

For the coupled spectrum some ten times as many scans were accumulated as for the broadband decoupled spectrum, although the concentration of **148** remained unchanged. This is apparent from the increased intensity of the solvent signal (septet for hexadeuterioacetone at  $\delta=29.3$ . The CO signal at  $\delta=206.3$  is not reproduced). The measurement of coupled spectra therefore requires a longer measurement time or a higher sample concentration. For a  $^1\text{H}$  broadband decoupled spectrum of a reasonably concentrated solution a few hundred or thousand scans are needed. To determine the time required it must be remembered that the signal:noise ratio  $S:N$  is proportional to  $\sqrt{n}$ , where  $n$  is the number of scans. The practical effect of this is that if the concentration is halved, then not twice as many, but four times as many scans are necessary to attain the same **signal:noise ratio**.

From the application of these considerations to the acquisition of fully coupled spectra, it can be appreciated that at least 10 times as many scans will be required as for a  $^1\text{H}$  broadband decoupled spectrum.

### 4.2 <sup>13</sup>C Chemical Shifts

In the introductory Sec. 1.2 (p. 73) the relationship between the **chemical shift** of a nucleus and the **shielding constant**  $\sigma$  was described.

$$10^{-6} \cdot \delta(X) = \sigma(\text{TMS}) - \sigma(X)$$

$$\sigma = \sigma_a + \sigma_b + \sigma'$$

In contrast to <sup>1</sup>H NMR the  $\sigma_{\text{para}}$  term is particularly important in <sup>13</sup>C NMR. Since this term involves **electronic excitation**, the

necessary energy  $\Delta E$  is involved in  $\sigma_{\text{para}}$ . With decreasing  $\Delta E$  a low field shift is observed.

The **hybridisation** of a <sup>13</sup>C atom is of decisive importance for the chemical shift. *sp*<sup>3</sup> C atoms absorb at highest field, followed by *sp* C atoms and finally by *sp*<sup>2</sup> C atoms at lowest field. This order is the same as for <sup>1</sup>H shifts of saturated, acetylenic, and olefinic protons. The shifts of <sup>13</sup>C nuclei and the protons attached to them often show parallel behaviour. This comparison should not however be taken too far. The <sup>13</sup>C and <sup>1</sup>H shifts of cyclobutane (**149**) and cyclopropane (**93**) for example do show parallel behaviour.

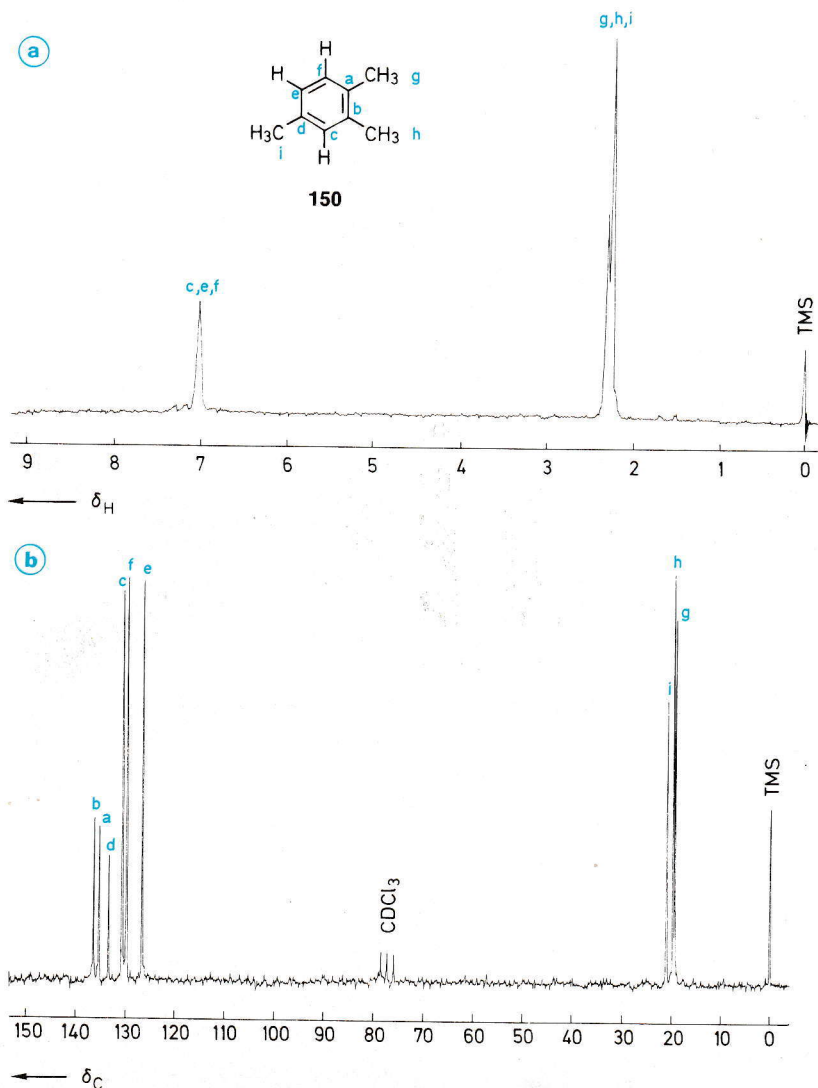


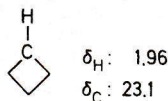
**Fig. 3.64** NMR spectra of 1,2,4-trimethylbenzene (**150**) in CDCl<sub>3</sub>

**a** <sup>1</sup>H spectrum

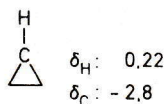
**b** <sup>13</sup>C spectrum (broadband decoupled)

$\delta$ a	135.0	f	129.5
b	136.2	g	19.2
c	130.5	h	19.5
d	133.1	i	20.8
e	126.5		



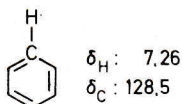


149

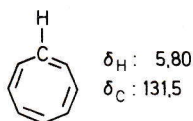


93

Benzene (75) and cyclooctatetraene (90) show opposite effects.



75



90

The **ring current**, a special case of an anisotropy effect, causes a marked low field shift in the  $^1\text{H}$  NMR of aromatics as compared to olefinic protons. In  $^{13}\text{C}$  NMR this effect is apparently negligible for the ring carbon atoms. Olefinic and aromatic carbons absorb in the same region. In the example above the  $^{13}\text{C}$  shift of cyclooctatetraene is even 3 ppm to low field of that of benzene. Since a comparison of  $^1\text{H}$  and  $^{13}\text{C}$  shifts shows that the **shift range** of  $^{13}\text{C}$ , ignoring extreme cases, is some 200 ppm whereas the  $^1\text{H}$  range is only some 10 ppm, it is apparent that changes in the chemical environment will in general be more noticeable in  $^{13}\text{C}$  than in  $^1\text{H}$  NMR. As an example the spectra of 1,2,4-trimethylbenzene (150) are reproduced (Fig. 3.64). Whereas in the  $^1\text{H}$  spectrum the three chemically non-equivalent ring protons overlap, and the three different methyl groups are very close together, well separated signals are observed in the  $^{13}\text{C}$  spectrum.

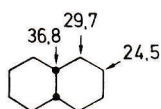
The value of  $^{13}\text{C}$  spectroscopy is particularly apparent for more complex molecules, for example steroids and alkaloids. In Fig. 3.65 quinine (151) is shown as an example. The twenty  $^{13}\text{C}$  signals for the twenty different C atoms are easily distinguished.

Functional groups generally deshield the  $^{13}\text{C}$  nucleus they are directly bound to. (A high field shift is however observed for heavy atoms such as iodine (155).) In the neighbouring  $\beta$ -position the deshielding is usually less. There are however exceptions, as shown by a comparison of 1-octanol (152) and 1-octanethiol (153):

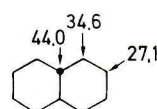
	$\alpha$	$\beta$	$\gamma$	$\delta$	$\epsilon$				
	X—CH <sub>2</sub>	—CH <sub>2</sub>	—CH <sub>2</sub>	—CH <sub>2</sub>	—CH <sub>2</sub>	—CH <sub>2</sub>	—CH <sub>2</sub>	—CH <sub>2</sub>	—CH <sub>3</sub>
152	(X = OH):	63.1	32.9	25.9	29.5	29.4	31.9	22.8	14.1
153	(X = SH):	24.7	34.2	28.5	29.2	29.1	31.9	22.8	14.1
154	(X = Br):	33.8	33.0	28.3	28.8	29.2	31.8	22.7	14.1
155	(X = I):	6.9	33.7	30.6	28.6	29.1	31.8	22.7	14.1

Iodine causes a low field shift in the  $\beta$ -position. (Compare C-1 with C-8, C-2 with C-7, etc.) The effect of substituents is not restricted, as in  $^1\text{H}$  NMR, to the immediate vicinity of the measured nucleus, but also includes more distant groups.

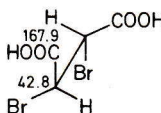
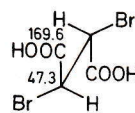
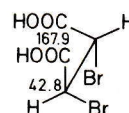
All X substituents cause an increase of the shielding of the  $\gamma$ -C atom of the carbon chain. The resulting high field shift is known as the  $\gamma$ -effect. The substituent effect on the  $\delta$  or farther positions is small in open chain compounds, but not necessarily in bi- and polycyclic compounds. Steric factors also play an important role, as shown by the examples of *cis*-decalin (156) and *trans*-decalin (157) and the stereoisomers of 2,3-dibromosuccinic acid (158–160). The enantiomers *RR* and *SS* with  $\text{C}_2$  symmetry have identical  $^{13}\text{C}$  spectra in an achiral medium; the achiral *meso*-form with a centre of symmetry has different shifts.



156



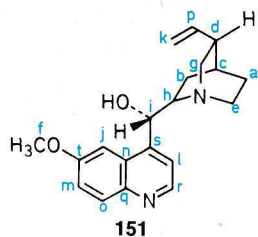
157


 158  
*RR* ( $\text{C}_2$ )

 159  
*meso* ( $\text{C}_i$ )

 160  
*SS* ( $\text{C}_2$ )

In the case of *geminal* multiple substitution the deshielding effects are not necessarily additive. A comparison of the shifts of the halogenomethanes shows that an increasing number of fluoro- or chloro-substituents causes an increasing low field shift. With increasing substitution with iodine the reverse effect, a high field shift, is observed. The trend for brominated methanes is inconsistent (Tab. 3.25).

Increasing alkyl substitution generally leads to a low field shift.

$$\delta(\text{CH}_4) < \delta(\text{C}_{\text{prim}}) < \delta(\text{C}_{\text{sec}}) < \delta(\text{C}_{\text{tert}}) < \delta(\text{C}_{\text{quart}})$$



a	21.6	h	60.1	o	131.1
b	27.7	i	71.8	p	141.9
c	27.9	j	101.6	q	143.9
d	40.0	k	114.2	r	147.2
e	43.2	l	118.4	s	148.5
f	55.6	m	121.2	t	157.6
g	57.0	n	126.6		

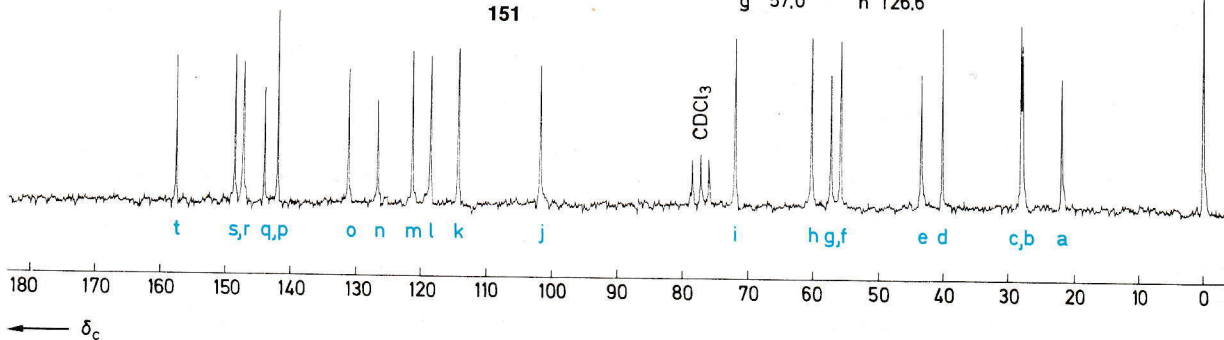


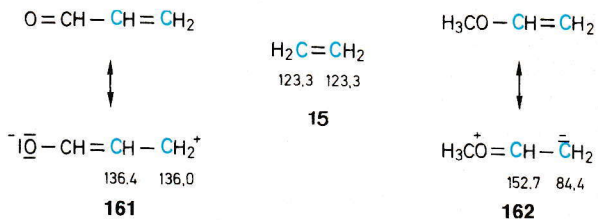
**Fig. 3.65** <sup>13</sup>C NMR spectra of quinine (**151**) in CDCl<sub>3</sub> (<sup>1</sup>H broadband decoupled)

**Tab. 3.25** Relationship between <sup>1</sup>J(C,H) and s-character of the hybrid orbitals of carbon

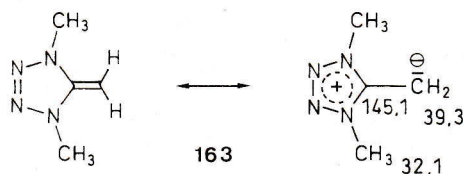
Compound	X=F	Cl	Br	I
CH <sub>3</sub> X	75.0	24.9	9.8	— 20.8
CH <sub>2</sub> X <sub>2</sub>	109.0	54.0	21.4	— 54.0
CHX <sub>3</sub>	116.4	77.0	12.1	— 139.9
CX <sub>4</sub>	118.6	96.5	— 29.0	— 292.5

The magnitude of the substituent effect is, as in <sup>1</sup>H NMR, dependent on the electronegativity of the substituent X. With increasing negativity of X the α-C atom is shifted further to low field. Tab. 3.25 shows this in the halogenated methane series. This rule no longer holds for the β-position and more distant carbons. The γ-effect in haloalkanes is exactly reversed. Fluorine causes the strongest high field shift, iodine the weakest.

Independent of the various factors which determine <sup>13</sup>C shifts there is a direct correlation between the δ values and the **charge density** at the relevant C atom. This relationship is very useful in spectral interpretation and will therefore be illustrated by some examples. If for example ethylene is compared with its formyl or methoxy derivatives, effects are observed which are typical for unsaturated carbonyl compounds (e.g. acrolein, **161**) and enol ethers (e.g. methyl vinyl ether, **162**):

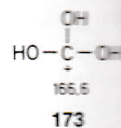
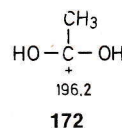
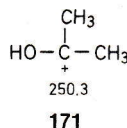
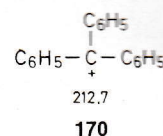
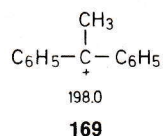
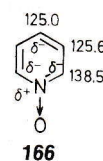
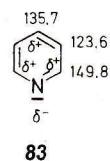
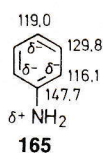
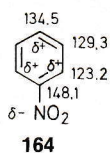


While the inductive effect is largely effective in the α-position, the mesomeric effect in the β-position causes a reduction of the electron density in acrolein (**161**) and an increase in methyl vinyl ether (**162**). The stronger deshielding is apparent as a low field shift, the stronger shielding as a high field shift. Extreme cases are observed for keteneacetals and related compounds:



Further examples are nitrobenzene (**164**) and aniline (**165**). As a result of the mesomeric effect the electron density in the o- and p-positions is changed. The same considerations can be applied to pyridine (**83**) and its N-oxide (**166**). The influence of charge density on <sup>13</sup>C shifts is clearly apparent. The shift of the o-C atoms in nitrobenzene (**164**) however also shows clearly that other factors need to be considered.





The relationship between  $^{13}\text{C}$  shift and electron density is particularly noticeable for ions. In Fig. 3.66 this is demonstrated using a comparison between uncharged benzene and aromatic ions as an example.

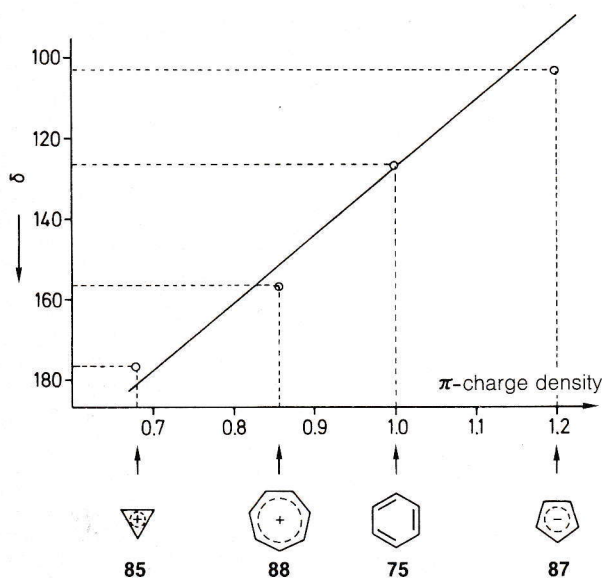
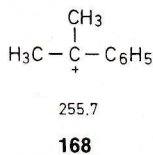
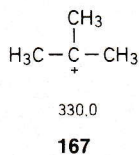
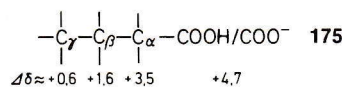
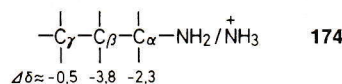


**Fig. 3.66** Relationship between  $^{13}\text{C}$  shifts and  $\pi$ -electron density in ions

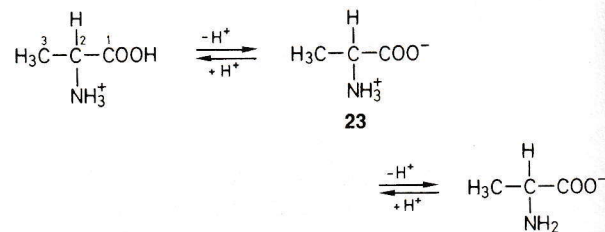
In studies of carbocations the measurement of their  $^{13}\text{C}$  spectra in "magic acid" played a decisive role. As shown by the examples (167–173), the extent of delocalisation of the charge is easily recognised from the  $^{13}\text{C}$  shift of the central C atom.



After these comments about the effect of charges on chemical shift it is understandable that the signals of acidic or basic compounds will be strongly pH dependent. Simplified assumptions of electron densities can however easily lead to errors. The protonation of linear alkyl amines generally causes a high-field shift of  $\text{C}_\alpha$ ,  $\text{C}_\beta$ , and  $\text{C}_\gamma$ ; conversely a low field shift is observed on deprotonation of carboxylic acids!



In the amphoteric amino acids the  $\delta$  values generally increase as the pH increases, as shown by the example of alanine:



pH	0.43	4.96	12.52
C-1	174.0	177.0	185.7
C-2	50.1	51.9	52.7
C-3	16.5	17.5	21.7

To conclude this section a few comments about **medium effects** on  $^{13}\text{C}$  shifts are appropriate. These can be described by an additional shielding constant  $\delta_{\text{Med}}$ . Where there are no special interactions, such as acidbase activity, solvent and concentration shifts are generally less than 3 ppm (see however the section on p. 171 on shift reagents).

The influence of temperature on <sup>13</sup>C shifts is also small, unless temperature-dependent processes (internal molecular motion, chemical rearrangements) alter the molecular structure (see Sec. 2, p. 86 ff.).

Tab. 3.26 shows measured coupling constants and values calculated from this formula for ethane, ethylene, and acetylene.

### 4.3 <sup>13</sup>C, <sup>1</sup>H Couplings

The coupling <sup>1</sup>J(C,H) is a measure of the s-character of the hybrid orbitals of the relevant C–H bonds. The following empirical relation holds approximately

$${}^1J(\text{C,H}) = 500 p \quad \text{with } p = \begin{cases} 0.25 \text{ for C} - sp^3 \\ 0.33 \text{ for C} - sp^2 \\ 0.50 \text{ for C} - sp \end{cases}$$

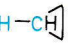
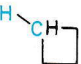
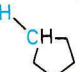
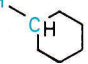
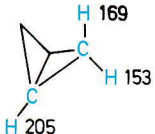
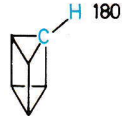
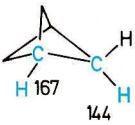
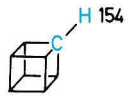
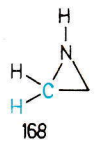
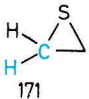
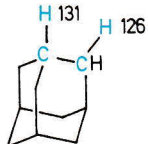
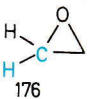
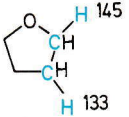
**Tab. 3.26** Relationship between <sup>1</sup>J(C,H) and s-character of the hybrid orbitals of carbon

Compound	Hybridisation <i>sp</i> <sup>λ<sup>2</sup></sup>	$p = \frac{1}{1 + \lambda^2}$		<sup>1</sup> J(C,H)	
		$\lambda^2$	$p$	calculated	measured
Ethane	<i>sp</i> <sup>3</sup>	3	0.25	125	124.9
Ethylene	<i>sp</i> <sup>2</sup>	2	0.33	167	156.4
Acetylene	<i>sp</i>	1	0.50	250	248

**Tab. 3.27** <sup>1</sup>J(C,H) coupling constants in substituted methanes

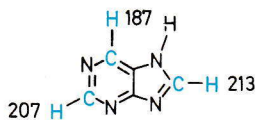
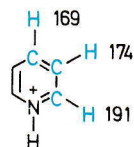
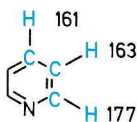
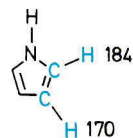
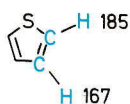
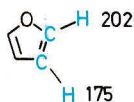
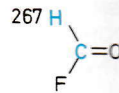
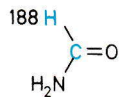
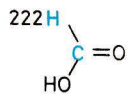
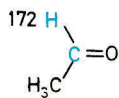
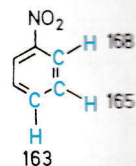
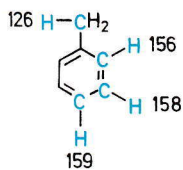
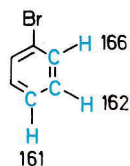
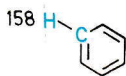
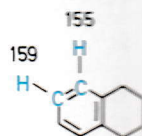
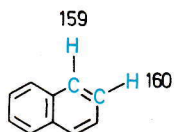
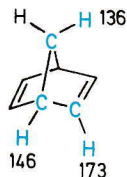
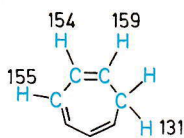
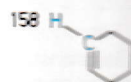
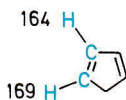
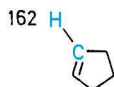
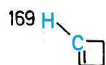
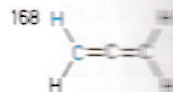
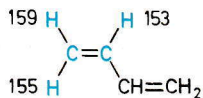
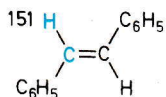
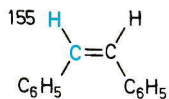
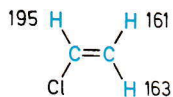
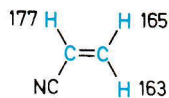
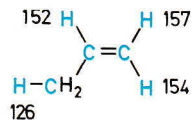
Compound	<sup>1</sup> J(C,H) (Hz)
CH <sub>4</sub>	125
CH <sub>3</sub> F	149
CH <sub>3</sub> Cl	150
CH <sub>3</sub> Br	152
CH <sub>3</sub> I	151
CH <sub>3</sub> NH <sub>2</sub>	133
CH <sub>3</sub> N <sup>+</sup> H <sub>3</sub>	145
CH <sub>3</sub> NO <sub>2</sub>	147
CH <sub>3</sub> OH	141
CH <sub>3</sub> O <sup>-</sup>	131
CH <sub>3</sub> OCH <sub>3</sub>	140
CH <sub>3</sub> SCH <sub>3</sub>	138
CH <sub>3</sub> Si(CH <sub>3</sub> ) <sub>3</sub>	118
CH <sub>3</sub> Li	98
CH <sub>2</sub> Cl <sub>2</sub>	177
CHCl <sub>3</sub>	209
CHF <sub>3</sub>	239

**Tab. 3.28** <sup>1</sup>J(C,H) couplings of selected compounds

Compound	<sup>1</sup> J(C,H) (Hz)
H–CH <sub>2</sub> –CH <sub>3</sub>	125
H–CH(CH <sub>3</sub> ) <sub>2</sub>	119
H–C(CH <sub>3</sub> ) <sub>3</sub>	114
H–CH <sub>2</sub> –CH=CH <sub>2</sub>	122
H–CH <sub>2</sub> –C <sub>6</sub> H <sub>5</sub>	129
H–CH <sub>2</sub> –C≡CH	132
H–CH <sub>2</sub> –C≡N	136
H–CH <sub>2</sub> –COOH	130
H–CH(OH)–C <sub>6</sub> H <sub>5</sub>	140
	160
	134
	128
	125
	
	
	
	
	
	
	
	
	



Tab. 3.28 continued

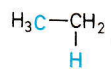
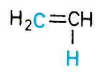
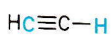
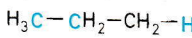
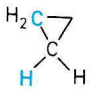
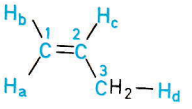
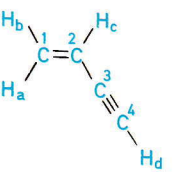
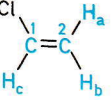
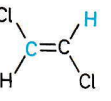
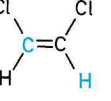
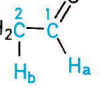
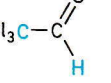


If the <sup>1</sup>J(C,H) coupling constants of cyclohexane (125 Hz) and cyclopropane (160 Hz) are compared, the similarity of cyclopropane to olefinic systems, as suggested by the Walsh orbital model, for example, is apparent. These estimates of s-character

of hybrid orbitals should however be restricted to hydrocarbons.

The effect of substituents on the <sup>1</sup>J(C,H) couplings constants is shown in Tab. 3.27 for a series of methane derivatives.

**Tab. 3.29** <sup>2</sup>J(C,H)-, <sup>3</sup>J(C,H)-, and higher couplings of selected compounds

Compound	<sup>2</sup> J(C,H) (Hz)	<sup>3</sup> J(C,H) (Hz)	<sup>n</sup> J(C,H) (Hz)
	-4.5		
	-2.4		
	+49.6		
	-4.4	+5.8	
	-2.5		
	C <sub>1</sub> H <sub>c</sub> : +0.4 C <sub>2</sub> H <sub>a</sub> : -2.6 C <sub>2</sub> H <sub>b</sub> : -1.2 C <sub>2</sub> H <sub>d</sub> : -6.8 C <sub>3</sub> H <sub>c</sub> : +5.0	C <sub>1</sub> H <sub>d</sub> : +6.7 C <sub>3</sub> H <sub>a</sub> : +7.6 C <sub>3</sub> H <sub>b</sub> : +12.7	
	C <sub>1</sub> H <sub>c</sub> : +8.8 C <sub>2</sub> H <sub>a</sub> : -3.7 C <sub>2</sub> H <sub>b</sub> : -0.3 C <sub>3</sub> H <sub>c</sub> : +2.0	C <sub>2</sub> H <sub>d</sub> : +4.8 C <sub>3</sub> H <sub>a</sub> : +9.5 C <sub>3</sub> H <sub>b</sub> : +16.3	C <sub>1</sub> H <sub>d</sub> : +2.8 (n = 4) C <sub>4</sub> H <sub>a</sub> : <1 (n = 4) C <sub>4</sub> H <sub>b</sub> : <1 (n = 4)
	C <sub>1</sub> H <sub>a</sub> : -8.3 C <sub>1</sub> H <sub>b</sub> : +7.1 C <sub>2</sub> H <sub>c</sub> : +6.8		
	+0.8		
	+16.0		
	C <sub>1</sub> H <sub>b</sub> : -6.6 C <sub>2</sub> H <sub>a</sub> : +26.7		
	+46.3		



Tab. 3.29 continued

Compound	${}^2J(\text{C,H})$ (Hz)	${}^3J(\text{C,H})$ (Hz)	${}^nJ(\text{C,H})$ (Hz)
	$\text{CH}_o$ : +1.1	$\text{CH}_m$ : +7.6	$\text{CH}_p$ : -1.2 ( $n = 4$ )
	$\text{C}_1\text{H}_a$ : -3.4 $\text{C}_2\text{H}_b$ : +1.4 $\text{C}_3\text{H}_a$ : +0.3 $\text{C}_3\text{H}_c$ : +1.6 $\text{C}_4\text{H}_b$ : +0.9	$\text{C}_1\text{H}_b$ : +11.1 $\text{C}_2\text{H}_c$ : +7.8 $\text{C}_2\text{H}'_a$ : +5.1 $\text{C}_3\text{H}'_b$ : +8.2 $\text{C}_4\text{H}_a$ : +7.4	$\text{C}_1\text{H}_c$ : -2.0 ( $n = 4$ ) $\text{C}_2\text{H}'_b$ : -1.2 ( $n = 4$ ) $\text{C}_3\text{H}'_a$ : -0.9 ( $n = 4$ )
		$\text{CH}_o$ : +4.1	$\text{CH}_m$ : +1.1 ( $n = 4$ ) $\text{CH}_p$ : +0.5 ( $n = 5$ )
	$\text{C}_2\text{H}_b$ : +7.4 $\text{C}_3\text{H}_a$ : +4.7 $\text{C}_3\text{H}'_b$ : +5.9	$\text{C}_2\text{H}'_b$ : +10.0 $\text{C}_2\text{H}'_a$ : +5.0 $\text{C}_3\text{H}'_a$ : +9.8	
	$\text{C}_2\text{H}_b$ : +3.1 $\text{C}_3\text{H}_a$ : +8.5 $\text{C}_3\text{H}_c$ : +0.9 $\text{C}_4\text{H}_b$ : +0.7	$\text{C}_2\text{H}'_a$ : +11.1 $\text{C}_2\text{H}_c$ : +6.8 $\text{C}_3\text{H}'_b$ : +6.6 $\text{C}_4\text{H}_a$ : +6.4	$\text{C}_2\text{H}'_b$ : -0.9 ( $n = 4$ ) $\text{C}_3\text{H}'_a$ : -1.7 ( $n = 4$ )

Since  ${}^1J(\text{C,H})$  is of some importance for spectral interpretation, some further examples are given in Tab. 3.28.

Whereas the  ${}^1J(\text{C,H})$  coupling constants lie between ca. +320 and +100 Hz, values of  ${}^2J(\text{C,H})$  between ca. +70 and -20 are

known. The *vicinal* couplings  ${}^3J(\text{C,H})$  are always positive and less than 15 Hz. Their values depend on the dihedral angle according to the Karplus curve (see p. 108). Some characteristic data for  ${}^2J(\text{C,H})$ ,  ${}^3J(\text{C,H})$ , and  ${}^nJ(\text{C,H})$  ( $n \geq 4$ ) are given in Tab. 3.29.

#### 4.4 Coupling of ${}^{13}\text{C}$ to Other Nuclei (D,F,N,P)

In Tab. 3.24 a series of  ${}^1J(\text{C,D})$  coupling constants have already been given for deuteriated solvents. Approximately,

$$J(\text{C,H}) : J(\text{C,D}) \approx \gamma_{\text{H}} : \gamma_{\text{D}} \approx 6.5 : 1$$

The  ${}^{13}\text{C,D}$  couplings are therefore considerably smaller than the corresponding  ${}^{13}\text{C,H}$  couplings.

Fig. 3.67 (see p. 153) shows the  ${}^{13}\text{C}$  spectrum of trifluoroacetic acid (176) in deuteriochloroform.

The direct  ${}^{13}\text{C},{}^{19}\text{F}$  couplings have a larger magnitude than the comparable  ${}^{13}\text{C},{}^1\text{H}$  couplings, but have a negative sign. The  ${}^1J(\text{C,F})$  values lie between -150 and -400 Hz. A selection of  ${}^nJ(\text{C,F})$  coupling constants is given in Tab. 3.30.

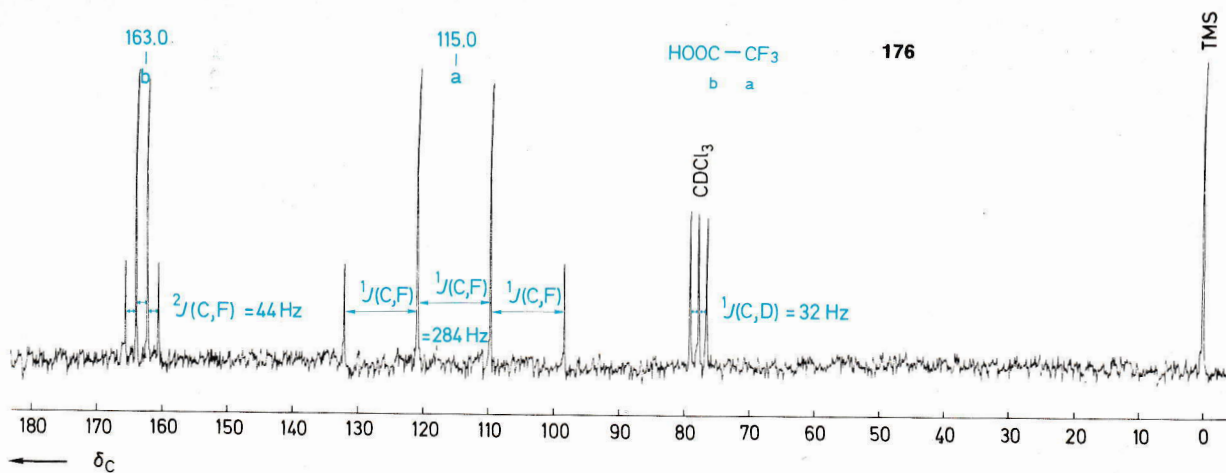


**Fig. 3.67** <sup>13</sup>C NMR spectra of trifluoroacetic acid (**176**) in deuteriochloroform

**Tab. 3.30** <sup>1</sup>J(C,F) coupling constants of selected compounds (in Hz)

Compound	<sup>1</sup> J(C,F)	<sup>2</sup> J(C,F)	<sup>n</sup> J(C,F)
F-CH <sub>3</sub>	162		
F-CFH <sub>2</sub>	235		
F-CF <sub>2</sub> H	274		
F-CF <sub>3</sub>	259		
F-CF <sub>2</sub> -C(OH) <sub>2</sub> -CF <sub>3</sub>	286	34	
F-CH <sub>2</sub> -CH <sub>2</sub> -CH <sub>2</sub> -C <sub>3</sub> H <sub>7</sub>	167	20	<sup>3</sup> J(C,F): 5 <sup>4</sup> J(C,F): < 2 <sup>5</sup> J(C,F): ≈ 0
F <sub>2</sub> C=CH <sub>2</sub>	287		
F <sub>2</sub> C=O	369		
F-CH <sub>2</sub> -CH <sub>2</sub> -CH <sub>2</sub> -CH <sub>2</sub> -CH <sub>2</sub> -CH <sub>2</sub> -F	171	19	<sup>3</sup> J(C,F): 5 <sup>4</sup> J(C,F): ≈ 0
F-C <sub>6</sub> H <sub>5</sub>	245	21	<sup>3</sup> J(C,F): 8 <sup>4</sup> J(C,F): 3
F-CF <sub>2</sub> -C <sub>6</sub> H <sub>5</sub>	272	32	<sup>3</sup> J(C,F): 4 <sup>4</sup> J(C,F): 1 <sup>5</sup> J(C,F): 0



**Tab. 3.31**  $^{13}\text{C}$ ,  $^{15}\text{N}$  coupling constants of selected compounds (in Hz)

Compound	$ ^1J(\text{C,N}) $	$ ^2J(\text{C,N}) $	$ ^nJ(\text{C,N}) $
$\text{H}_3\text{C}-\text{NH}_2$	5		
$\text{H}_3\text{C}-\overset{+}{\text{N}}(\text{CH}_3)_3$	6		
	14	10	
$\text{H}_3\text{C}-\text{C}\equiv\text{N}$	18	3	
	11.4	2.7	$^3J(\text{C,N}): 1,3$ $^4J(\text{C,N}): < 1$
	0.5	2.4	$^3J(\text{C,N}): 3,9$
	12.0	2.1	$^3J(\text{C,N}): 5,3$

A few comments on  $^{13}\text{C}$ ,  $^{15}\text{N}$  and  $^{13}\text{C}$ ,  $^{31}\text{P}$  couplings will complete this section. Whereas  $^{13}\text{C}$ ,  $^{19}\text{F}$  and  $^{13}\text{C}$ ,  $^{31}\text{P}$  couplings can be directly measured from  $^1\text{H}$  broadband decoupled  $^{13}\text{C}$  spectra,  $^{13}\text{C}$ ,  $^{15}\text{N}$  couplings are only accessible *via*  $^{15}\text{N}$  enrichment. The natural abundance of both  $^{19}\text{F}$  and  $^{31}\text{P}$  is 100%, but only 0.37% for  $^{15}\text{N}$  (see Tab. 3.1, p. 72). Some idea of typical values of  $^{13}\text{C}$ ,  $^{15}\text{N}$  and  $^{13}\text{C}$ ,  $^{31}\text{P}$  coupling constants can be gained from the examples given in Tabs. 3.31 and 3.32.

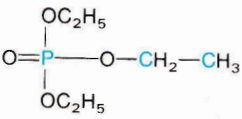
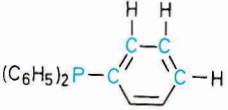
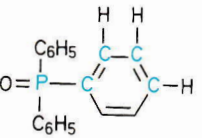
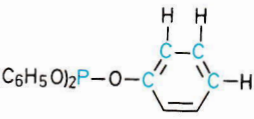
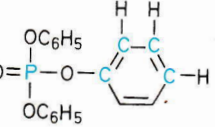
#### 4.5 $^{13}\text{C}$ , $^{13}\text{C}$ Couplings

The coupling of a  $^{13}\text{C}$  nucleus with a neighbouring  $^{13}\text{C}$  nucleus is generally not observable in routine  $^{13}\text{C}$  NMR spectra. The low natural abundance of  $^{13}\text{C}$  of 1.1% means that the nuclear combination  $^{13}\text{C}\dots^{13}\text{C}$  is only ca. 1/100 times as likely as  $^{13}\text{C}\dots^{12}\text{C}$  and only  $10^{-4}$  times as likely as  $^{12}\text{C}\dots^{12}\text{C}$ . Apart from weak satellites in long accumulations of intense signals of pure liquids the measurement of  $^{13}\text{C}$ ,  $^{13}\text{C}$  couplings requires the use of  $^{13}\text{C}$  enriched compounds or the use of the INADEQUATE method (see p. 179).

**Tab. 3.32**  $^{13}\text{C}$ ,  $^{31}\text{P}$  coupling constants of selected compounds (in Hz)

Compound	$ ^1J(\text{C,P}) $	$ ^2J(\text{C,P}) $	$ ^nJ(\text{C,P}) $
$\text{P}(\text{CH}_2-\text{CH}_2-\text{CH}_2-\text{CH}_3)_3$	11	12	$^3J(\text{C,P}): 13$ $^4J(\text{C,P}): \approx 0$
$^+\text{P}(\text{CH}_2-\text{CH}_2-\text{CH}_2-\text{CH}_3)_4 \text{Br}^-$	48	4	$^3J(\text{C,P}): 15$ $^4J(\text{C,P}): \approx 0$
$\text{Cl}_2\text{P}-\text{CH}_2-\text{CH}_2-\text{CH}_2-\text{CH}_3$	44	14	$^3J(\text{C,P}): 11$ $^4J(\text{C,P}): \approx 0$
$\text{O}=\text{P}(\text{CH}_2-\text{CH}_2-\text{CH}_2-\text{CH}_3)_3$	66	5	$^3J(\text{C,P}): 13$ $^4J(\text{C,P}): \approx 0$
	141	5	$^3J(\text{C,P}): 16$ $^4J(\text{C,P}): 1$ $^{5,6}J(\text{C,P}): \approx 0$
	300	53	$^3J(\text{C,P}): 5$
$(\text{H}_5\text{C}_2\text{O})_2\text{P}-\text{O}-\text{CH}_2-\text{CH}_3$		11	$^3J(\text{C,P}): 5$

Tab. 3.32 continued

Compound	<sup>1</sup> J(C,P)	<sup>2</sup> J(C,P)	<sup>n</sup> J(C,P)
		6	<sup>3</sup> J(C,P): 7
	13	20	<sup>3</sup> J(C,P): 7 <sup>4</sup> J(C,P): 0.3
	104	10	<sup>3</sup> J(C,P): 12 <sup>4</sup> J(C,P): 2
		3	<sup>3</sup> J(C,P): 7 <sup>4</sup> J(C,P): ≈0 <sup>5</sup> J(C,P): 1
		7	<sup>3</sup> J(C,P): 5 <sup>4</sup> J(C,P): 1 <sup>5</sup> J(C,P): 2

<sup>13</sup>C, <sup>13</sup>C couplings show a similar dependence on hybridisation and electronic effects as <sup>1</sup>H, <sup>13</sup>C couplings.

The following series of compounds shows that <sup>1</sup>J(C,C) increases strongly with the s-character of the orbitals involved:

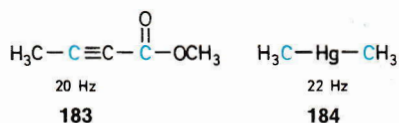
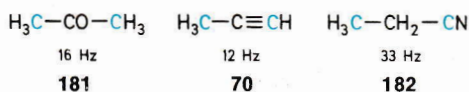
<i>sp-sp</i>	$\left\{ \begin{array}{l} \text{HC}\equiv\text{C}-\text{C}\equiv\text{CH} \\ \text{HC}\equiv\text{CH} \\ \text{HC}\equiv\text{C}-\text{C}\equiv\text{CH} \end{array} \right.$	+ 190.3 Hz	<b>177</b>	$\left. \begin{array}{l} \text{sp}^2\text{-sp}^2 \\ \left\{ \begin{array}{l} \text{H} \quad \text{H} \\   \quad   \\ \text{C} \quad \text{C} \\   \quad   \\ \text{H}_2\text{C}=\text{CH}-\text{CH}=\text{CH}_2 \end{array} \right. \end{array} \right\}$	+ 56.0 Hz	<b>75</b>
		+ 171.5 Hz	<b>178</b>		+ 53.7 Hz	<b>118</b>
		+ 153.4 Hz	<b>177</b>			
<i>sp<sup>2</sup>-sp</i>	$\left\{ \begin{array}{l} \text{H}_2\text{C}=\text{C}=\text{CH}_2 \\ \text{HC}\equiv\text{C}-\text{CH}=\text{CH}_2 \end{array} \right.$	+ 98.7 Hz	<b>179</b>	$\left. \begin{array}{l} \text{sp}^3\text{-sp}^2 \\ \left\{ \begin{array}{l} \text{H}_3\text{C}-\text{C} \\   \\ \text{H}_3\text{C}-\text{CH}=\text{CH}_2 \end{array} \right. \end{array} \right\}$	+ 44.2 Hz	<b>77</b>
		+ 86.7 Hz	<b>180</b>		+ 41.9 Hz	<b>68</b>
<i>sp<sup>2</sup>-sp<sup>2</sup></i>	$\left\{ \begin{array}{l} \text{H}_2\text{C}=\text{CH}-\text{CH}=\text{CH}_2 \\ \text{H}_2\text{C}=\text{CH}_2 \end{array} \right.$	+ 68.6 Hz	<b>118</b>	$\left. \begin{array}{l} \text{sp}^3\text{-sp}^3 \\ \text{H}_3\text{C}-\text{CH}_3 \end{array} \right\}$	+ 34.6 Hz	<b>92</b>
		+ 67.6 Hz	<b>15</b>			
<i>sp<sup>3</sup>-sp</i>	$\text{H}_3\text{C}-\text{C}\equiv\text{CH}$	+ 67.4 Hz	<b>70</b>	$\left. \begin{array}{l} \text{H}_2\text{C} \triangle \text{CH}_2 \end{array} \right\}$	+ 12.4 Hz	<b>93</b>

The effect of substituents on <sup>1</sup>J(C,C) is generally small for saturated C atoms; larger effects are observed for olefinic, aromatic, or carbonyl carbons.



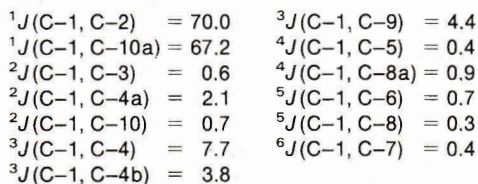
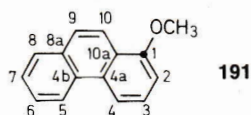
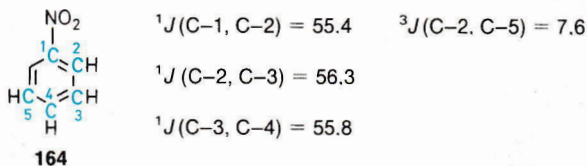
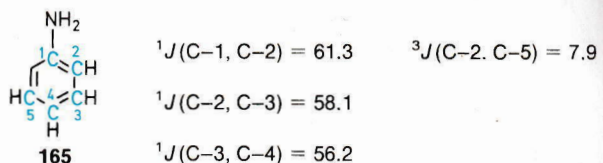
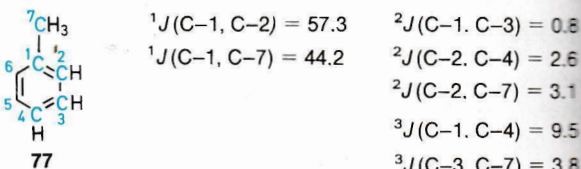
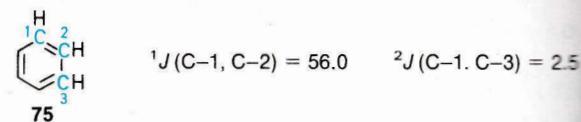
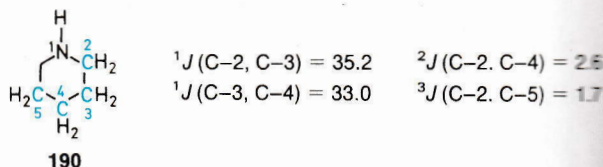
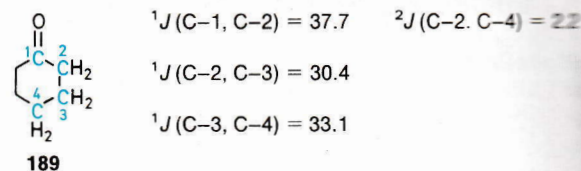
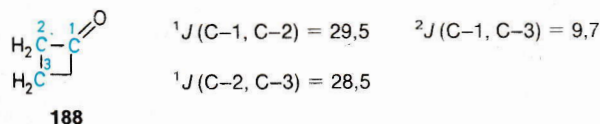
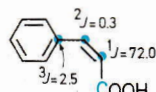
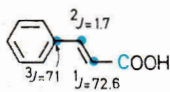
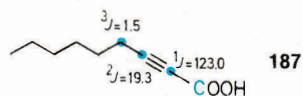
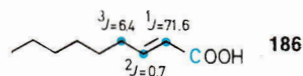
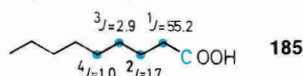
	X = H	CH <sub>3</sub>	Cl	OC <sub>2</sub> H <sub>5</sub>
H <sub>3</sub> C-CH <sub>2</sub> -X	34.6	34.6	36.1	38.9
H <sub>2</sub> C=CH-X	67.6	70.0	77.6	78.1
HC≡C-X	171.5	175.0		216.5
<hr/>				
C <sub>6</sub> H <sub>5</sub> -X	56.0	57.1	65.2	67.0
H <sub>3</sub> C-CO-X	39.4	40.1	56.1	58.8

Geminal couplings  $^2J(C,C)$  can be positive or negative; their magnitude is generally less than 5 Hz. Exceptions occur particularly for carbonyl compounds, alkynes, and organometallic compounds.



$^3J(C,C)$  coupling constants are positive and generally smaller than 5 Hz. Exceptions occur for conjugated systems; thus the  $^3J$  coupling between C-1 and C-4 in butadiene for example is 9.1 Hz.

A few further  $^{13}C$ ,  $^{13}C$  couplings (values in Hz) are tabulated below.



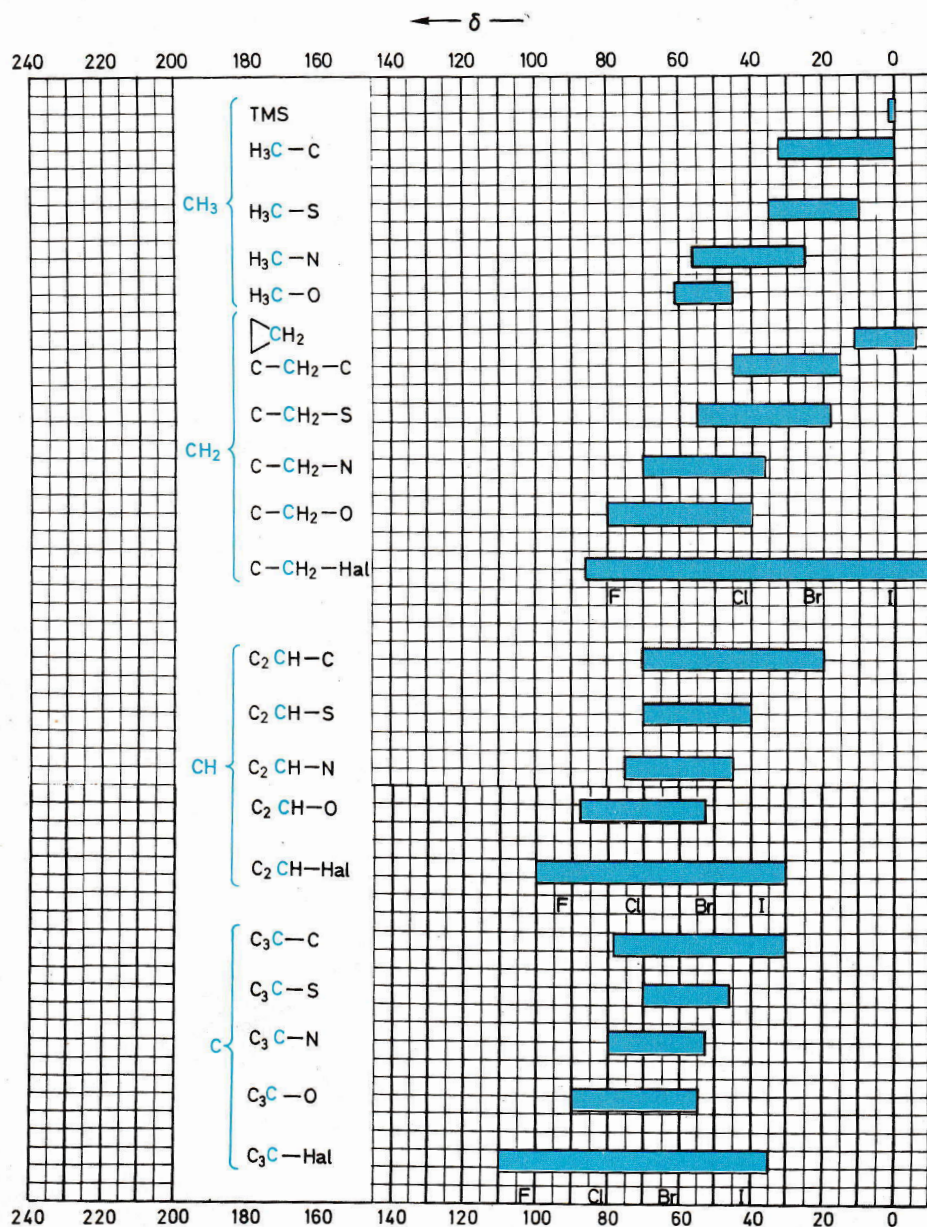
### 4.6 Correlation of <sup>13</sup>C Shifts With Structural Features

The ranges of the <sup>13</sup>C chemical shifts for the most important structural types of organic compounds are collected in Tab. 3.33. Extreme values are ignored. For the interpretation of <sup>13</sup>C

spectra it is recommended that this table is used in conjunction with the data in Sec. 5 (see p. 185) arranged by type of compound and the increment systems in Sec. 4.7 (see p. 159).

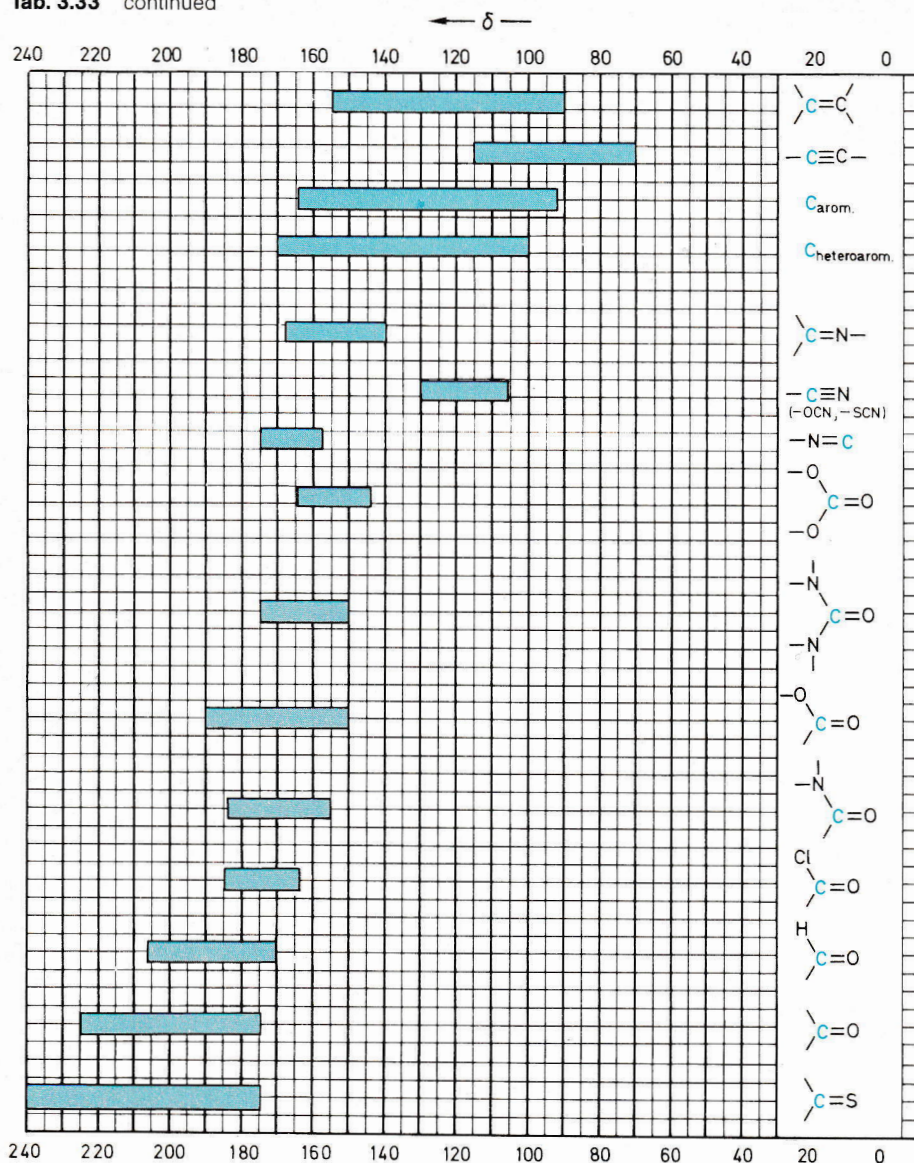
If more than one functional group is attached to a single saturated C atom, then to a first approximation the additivity of the shift effects can be assumed (see also Sec. 4.7).

Tab. 3.33 <sup>13</sup>C shifts of important structural elements; δ values (ppm)





Tab. 3.33 continued

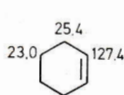
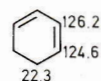
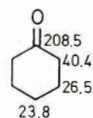
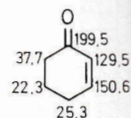


For the effect of functional groups on (C=C) bonds or aromatic rings see Sec. 4.2 (p. 145) and Sec. 4.7 (p. 159).

It is already apparent from the ranges given in Tab. 3.33 that the chemical shifts of carbonyl carbons vary greatly with the compound type. An explicit comparison is possible from the data in Tab. 3.34.

Conjugation of double bonds has relatively little effect, unless charge shifts are effective. Two examples underline this: cyclohexene (**107**)/1,3-cyclohexadiene (**74**) and cyclohexanone

(**189**)/2-cyclohexen-1-one (**192**).

**107****74****189****192**

Cumulated double bonds on the other hand lead to very characteristic  $\delta$ -values of the chemical shifts (Tab. 3.35).

**Tab. 3.34** <sup>13</sup>C shifts of carbonyl C-atoms in various types of compounds

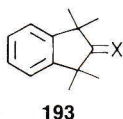
Type of compound	R—CO—X	δ values	
		R = CH <sub>3</sub>	R = C <sub>6</sub> H <sub>5</sub>
Ketones	R—CO—CH <sub>3</sub>	206.0	195.7
Aldehydes	R—CO—H	199.7	197.6
Thiocarboxylic acids			
S-esters	R—CO—SC <sub>2</sub> H <sub>5</sub>	195.0	191.2
Carboxylate salts	R—CO—O <sup>-</sup>	181.7	175.5
Carboxylic acids	R—CO—OH	178.1	172.6
Carboxylic acid amides	R—CO—NH <sub>2</sub>	172.7	169.7
Carboxylic acid esters	R—CO—OCH <sub>3</sub>	170.7	166.8
Carboxylic acid chlorides	R—CO—Cl	170.5	168.0
Carboxylic acid anhydrides	R—CO—OCOR	166.9	162.9

Type of compound	X—CO—X	δ values	
Ureas	R <sub>2</sub> N—CO—NR <sub>2</sub>	161.2 (R = H), 165.4 (R = CH <sub>3</sub> )	
Urethanes	RNH—CO—OR	157.8 (OR = OC <sub>2</sub> H <sub>5</sub> , NR = NCH <sub>3</sub> )	
Carbonate esters	RO—CO—OR	156.5 (R = CH <sub>3</sub> )	
Chloroformate esters	Cl—CO—OR	149.9 (R = C <sub>2</sub> H <sub>5</sub> )	
Phosgene	Cl—CO—Cl	142.1	

**Tab. 3.35** <sup>13</sup>C shifts of compounds with cumulated double bonds

Allene	$\text{H}_2\text{C}=\text{C}=\text{CH}_2$ 73.5 212.6
Ketene	$\text{H}_2\text{C}=\text{C}=\text{O}$ 2.5 194.0
Diazomethane	$\text{H}_2\text{C}=\text{N}=\text{N}$ 23.1
Methyl isocyanate	$\text{H}_3\text{C}-\text{N}=\text{C}=\text{O}$ 26.3 121.5
Methyl isothiocyanate	$\text{H}_3\text{C}-\text{N}=\text{C}=\text{S}$ 29.3 128.7
Dicyclohexylcarbodiimide	 25.5 55.8 139.9 24.8 35.0
Carbon dioxide	$\text{O}=\text{C}=\text{O}$ 123.9
Carbon disulfide	$\text{S}=\text{C}=\text{S}$ 192.3

Extreme shift values are observed for thio-, seleno-, and telluroketones.



x	δ
O	226
S	282
Se	294
Te	301

### 4.7 Increment Systems for the Estimation of <sup>13</sup>C Shifts

The <sup>13</sup>C shifts of aliphatic compounds and benzene derivatives can be estimated with **empirical increment systems**. If there is more than one substituent an additive behaviour is assumed. The following increment systems are a useful aid for the assignment of <sup>13</sup>C signals. The tabulated examples however show the possible deviations between calculated and observed shifts.

For the estimation of the <sup>13</sup>C shifts of saturated C atoms the simplest procedure is to base the calculation on a corresponding hydrocarbon and add the increments for the various functional groups.

If the <sup>13</sup>C shifts δ<sub>i</sub> of the hydrocarbon itself are not known, they can be calculated from the **Grant-Paul rules** as follows

$$\delta_i = -2.3 + \sum_k A_k n_k + S_{i\alpha}$$

The increments A<sub>k</sub>n<sub>k</sub> are added to the shift value for methane δ = 2.3. Increments are added for all the positions k = α, β, γ, δ, ε relative to the relevant carbon. n<sub>k</sub> is the number of C atoms at position k. The increments A<sub>k</sub> have the following values:

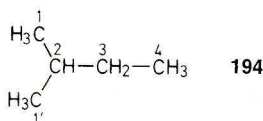
$$A_\alpha = +9.1 \quad A_\gamma = 2.5 \quad A_\epsilon = +0.2$$

$$A_\beta = +9.4 \quad A_\delta = +0.3$$

For tertiary and quaternary C atoms and their immediate neighbours a steric correction factor S<sub>iα</sub> must be added. This is derived from the most substituted carbon C<sub>α</sub> next to the carbon C<sub>i</sub> for which the shift is being calculated. The correction values S<sub>iα</sub> are then as follows.

C <sub>i</sub> (Carbon atom under consideration)	C <sub>α</sub> (highest substituted neighbouring C atom)	S <sub>iα</sub>			
		—CH <sub>3</sub>	—CH <sub>2</sub> —	—CH—	—C—
primary	—CH <sub>3</sub>	0	0	- 1.1	- 3.4
secondary	—CH <sub>2</sub> —	0	0	- 2.5	- 7.5
tertiary	—CH—	0	- 3.7	- 9.5	(- 15.0)
quaternary	—C—	- 1.5	- 8.4	(- 15.0)	(- 25.0)

The system will become clearer from a consideration of 2 methylbutane (**194**).





$C_i$	$-2.3$	$+\sum_k A_k n_k$	$+S_{i\alpha}$	$\equiv \delta_{\text{calculated}}$	$\delta_{\text{observed}}$
C-1	-2.3	+9.1 +9.4 · 2 -2.5	-1.1	= 22.0	21.9
C-2	-2.3	+9.1 · 3 +9.4	-3.7	= 30.7	29.7
C-3	-2.3	+9.1 · 2 +9.4 · 2	-2.5	= 32.2	31.7
C-4	-2.3	+9.1 +9.4 -2.5 · 2		= 11.2	11.4

In sterically hindered hydrocarbons the agreement between  $\delta_{\text{calculated}}$  and  $\delta_{\text{observed}}$  is poorer. If rotation around a C-C bond is restricted or prevented, then additional **conformational corrections** must be made.

**Tab. 3.36** Increment system for the estimation of  $^{13}\text{C}$  shifts of aliphatic compounds

$\delta_i(\text{RX}) = \delta_i(\text{RH}) + I_{ik} + S_{i\alpha}$  ( $k = \alpha, \beta, \gamma, \delta$ ) for all  $C_i$

Substituent X	$k = \alpha$	$\beta$	$\gamma$	$\delta$
$\begin{array}{c} \text{---C=C---} \\   \quad   \end{array}$	20.0	6.9	-2.1	0.4
$\text{---C}\equiv\text{C---}$	4.4	5.6	-3.4	-0.6
$\text{---C}_6\text{H}_5$	22.1	9.3	-2.6	0.3
$\text{---CH=O}$	29.9	-0.6	-2.7	0
$\text{---C=O}$	22.5	3.0	-3.0	0
$\begin{array}{c} \text{R} \\   \\ \text{---COOH} \\ \text{---COOR} \\ \text{---CO---NR}_2 \\ \text{---COCl} \\ \text{---C}\equiv\text{N} \end{array}$	20.1 22.6 22.0 33.1 3.1	2.0 2.0 2.6 2.3 2.4	-2.8 -2.8 -3.2 -3.6 -3.3	0 0 -0.4 0 -0.5
$\text{---OH}$	49.0	10.1	-6.2	0
$\text{---OR}$	58.0	7.2	-5.8	0
$\text{---O---CO---R}$	54.0	6.5	-6.0	0
$\text{---NR}_2$	28.3	11.3	-5.1	0
$\text{---NR}_3^+$	30.7	5.4	-7.2	-1.4
$\text{---NO}_2$	61.6	3.1	-4.6	-1.0
$\text{---SH}$	10.6	11.4	-3.6	-0.4
$\text{---SCH}_3$	20.4	6.2	-2.7	0
$\text{---F}$	70.1	7.8	-6.8	0
$\text{---Cl}$	31.0	10.0	-5.1	-0.5
$\text{---Br}$	18.9	11.0	-3.8	-0.7
$\text{---I}$	-7.2	10.9	-1.5	-0.9

**Tab. 3.37** Calculated and observed  $\delta$  values for selected aliphatic compounds

Compound	$\delta_{\text{calculated}}^a$	$\delta_{\text{observed}}$
1-Hexyne		
$\text{HC}\equiv\text{C}-\text{CH}_2-\text{CH}_2-\text{CH}_2-\text{CH}_3$		
C-1	-	67.4
C-2	-	82.8
C-3	17.4 (18.1)	17.4
C-4	30.4 (30.9)	29.9
C-5	21.4 (21.9)	21.2
C-6	12.4 (13.1)	12.9
Basis		
$\text{H}_3\text{C}-\text{CH}_2-\text{CH}_2-\text{CH}_3$		
C-1	13.7	13.0
C-2	25.3	24.8
2-Butanol <sup>b</sup>		
$\text{H}_3\text{C}-\text{CH}(\text{OH})-\text{CH}_2-\text{CH}_3$		
C-1	22.0 (22.7)	22.6
C-2	70.1 (70.6)	68.7
C-3	32.4 (32.9)	32.0
C-4	6.8 (7.5)	9.9
Basis		
$\text{H}_3\text{C}-\text{CH}_2-\text{CH}_2-\text{CH}_3$		
C-1	13.7	13.0
C-2	25.3	24.8
2-Chloro-2-methylbutane		
$\text{H}_3\text{C}-\text{C}(\text{Cl})(\text{CH}_3)-\text{CH}_2-\text{CH}_3$		
C-1	31.9 (32.0)	32.0
C-2	60.7 (61.7)	71.1
C-3	41.7 (42.2)	38.8
C-4	6.3 (6.1)	9.4
Basis		
$\text{H}_3\text{C}-\text{CH}(\text{CH}_3)-\text{CH}_2-\text{CH}_3$		
C-1	22.0	21.9
C-2	30.7	29.7
C-3	32.2	31.7
C-4	11.2	11.4
Leucine <sup>b</sup>		
$\text{HOOC}-\text{CH}(\text{NH}_2)-\text{CH}_2-\text{CH}(\text{CH}_3)-\text{CH}_3$		
C-1	-	176.6
C-2	56.1 (55.9)	54.8
C-3	42.5 (43.0)	41.0
C-4	21.8 (22.8)	25.4
C-5		
C-6	21.9 (22.0)	23.2/22.1
Basis		
$\text{H}_3\text{C}-\text{CH}(\text{CH}_3)-\text{CH}_2-\text{CH}_3$		
C-1	22.0	21.9
C-2	30.7	29.7
C-3	32.2	31.7
C-4	11.2	11.4

<sup>a</sup> The basis values used are the **observed**  $^{13}\text{C}$  shifts of the hydrocarbon; the  $\delta$  values in brackets are calculated from the **calculated**  $^{13}\text{C}$  shifts of the hydrocarbon

<sup>b</sup> For C-1, C-2 and C-3 in 2-butanol and for C-2 and C-3 in leucine steric correction factors  $S_{i\alpha}$  have been included

Using the measured or calculated  $\delta_i$  values of an alkane  $C_nH_{2n+2}$  as a basis the <sup>13</sup>C shifts of the substituted compounds  $C_nH_{2n+1}X$ ,  $C_nH_{2n}XY$ , etc. can be calculated. Tab. 3.36 gives the increments  $I$  for a selection of substituents  $X$  depending on the position of substitution relative to the carbon  $C_i$  for which the shift is being calculated.

In Tab. 3.37 the observed shifts of some representative examples are given, together with the values calculated with the increment system. (For the substituents  $-OR$ ,  $-NR_2$  and  $-SR$  it is recommended to apply the steric corrections  $S_{i\sigma}$  as for hydrocarbons.)

The <sup>13</sup>C shifts of olefinic carbons can be calculated using the values given in Tab. 3.38.

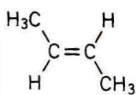
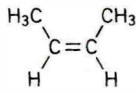
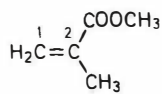
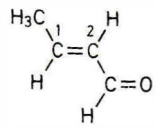
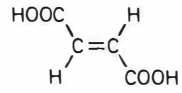
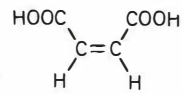
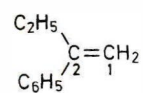
**Tab. 3.38** Increment system for the estimation of <sup>13</sup>C shifts of olefinic carbons

$X-\overset{1}{C}H=\overset{2}{C}H_2$	$\delta_1 = 123.3 + I_1$	$\delta_2 = 123.3 + I_2$
$X-\overset{1}{C}H=\overset{2}{C}H-Y$	$\delta_1 = 123.3 + I_{X1} + I_{Y2}$	$\delta_2 = 123.3 + I_{Y1} + I_{X2}$

Substituent	Increments	
	$I_1$	$I_2$
-H	0	0
-CH <sub>3</sub>	10.6	- 8.0
-C <sub>2</sub> H <sub>5</sub>	15.5	- 9.7
-CH <sub>2</sub> -CH <sub>2</sub> -CH <sub>3</sub>	14.0	- 8.2
-CH(CH <sub>3</sub> ) <sub>2</sub>	20.3	- 11.5
-(CH <sub>2</sub> ) <sub>3</sub> -CH <sub>3</sub>	14.7	- 9.0
-C(CH <sub>3</sub> ) <sub>3</sub>	25.3	- 13.3
-CH=CH <sub>2</sub>	13.6	- 7.0
-C≡C-R	7.5	8.9
-C <sub>6</sub> H <sub>5</sub>	12.5	- 11.0
-CH <sub>2</sub> Cl	10.2	- 6.0
-CH <sub>2</sub> Br	10.9	- 4.5
-CH <sub>2</sub> OR	13.0	- 8.6
-CH=O	13.1	12.7
-CO-CH <sub>3</sub>	15.0	5.9
-COOH	4.2	8.9
-COOR	6.0	7.0
-CN	- 15.1	14.2
<hr/>		
-OR	28.8	- 39.5
-O-CO-R	18.0	- 27.0
-NR <sub>2</sub>	16.0	- 29.0
-N <sup>+</sup> (CH <sub>3</sub> ) <sub>3</sub>	19.8	- 10.6
-NO <sub>2</sub>	22.3	- 0.9
-SR	19.0	- 16.0
<hr/>		
-F	24.9	- 34.3
-Cl	2.6	- 6.1
-Br	- 7.9	- 1.4
-I	- 38.1	7.0

Tab. 3.39 gives an impression of the "quality" of the estimations possible with this increment system. (The application of the system to trisubstituted olefins, not to mention tetrasubstituted olefins, is not recommended.)

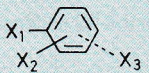
**Tab. 3.39** Calculated and observed  $\delta$  values for the <sup>13</sup>C shifts of olefinic C atoms

Compound	$\delta_i$ calculated		$\delta_i$ observed	
	C-1	C-2	C-1	C-2
2-Butene				
	125.9	125.9	124.8	124.8
	125.9	125.9	123.4	123.4
<hr/>				
Methyl methacrylate				
	122.3	139.9	124.7	136.9
<hr/>				
(E)-Crotonaldehyde				
	146.6	128.4	153.7	134.9
<hr/>				
Fumaric acid				
	136.4	136.4	134.5	134.5
Maleic acid				
	136.4	136.4	130.8	130.8
<hr/>				
2-Phenyl-1-butene				
	102.6	151.3	109.7	148.9



The increment system for benzene derivatives in Tab. 3.40 works on similar principles. The increments  $I_1, I_2$  etc. for each substituent  $X_1, X_2$  etc. are added to the basis value for benzene

**Tab. 3.40** Increment system for the estimation of  $^{13}\text{C}$  shifts of substituted benzenes



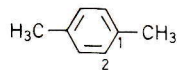
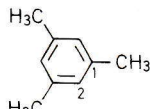
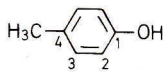
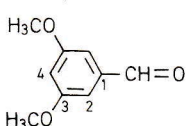
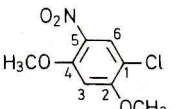
$$\delta_i = 128,5 + I_{1i} + I_{2i} + \dots$$

Substituent	ipso	ortho	meta	para
—H	0.0	0.0	0.0	0.0
—CH <sub>3</sub>	9.3	0.6	0.0	−3.1
—C <sub>2</sub> H <sub>5</sub>	15.7	−0.6	−0.1	−2.8
—CH(CH <sub>3</sub> ) <sub>2</sub>	20.1	−2.0	0.0	−2.5
—C(CH <sub>3</sub> ) <sub>3</sub>	22.1	−3.4	−0.4	−3.1
—CH=CH <sub>2</sub>	7.6	−1.8	−1.8	−3.5
—C≡CH	−6.1	3.8	0.4	−0.2
—C <sub>6</sub> H <sub>5</sub>	13.0	−1.1	0.5	−1.0
—CF <sub>3</sub>	2.6	−2.6	−0.3	−3.2
—CH <sub>2</sub> Cl	9.1	0.0	0.2	−0.2
—CH <sub>2</sub> Br	9.2	0.1	0.4	−0.3
—CH <sub>2</sub> OR	13.0	−1.5	0.0	−1.0
—CH <sub>2</sub> —NR <sub>2</sub>	15.0	−1.5	−0.2	−2.0
—CH=O	7.5	0.7	−0.5	5.4
—CO—CH <sub>3</sub>	9.3	0.2	0.2	4.2
<hr/>				
—COOH	2.4	1.6	−0.1	4.8
—COOR	2.0	1.0	0.0	4.5
—CO—NR <sub>2</sub>	5.5	−0.5	−1.0	5.0
—COCl	4.6	2.9	0.6	7.0
—C≡N	−16.0	3.5	0.7	4.3
<hr/>				
—OH	26.9	−12.6	1.6	−7.6
—OCH <sub>3</sub>	31.3	−15.0	0.9	−8.1
—OC <sub>6</sub> H <sub>5</sub>	29.1	−9.5	0.3	−5.3
—O—CO—R	23.0	−6.0	1.0	−2.0
<hr/>				
—NH <sub>2</sub>	19.2	−12.4	1.3	−9.5
—NR <sub>2</sub>	21.0	−16.0	0.7	−12.0
—NH—CO—CH <sub>3</sub>	11.1	−9.9	0.2	−5.6
—N=N—C <sub>6</sub> H <sub>5</sub>	24.0	−5.8	0.3	2.2
—N=C=O	5.7	−3.6	1.2	−2.8
—NO <sub>2</sub>	19.6	−5.3	0.8	6.0
<hr/>				
—SH	2.2	0.7	0.4	−3.1
—SCH <sub>3</sub>	10.1	−1.6	0.2	−3.5
—SC <sub>6</sub> H <sub>5</sub>	6.8	0.5	2.2	−1.6
—SO <sub>3</sub> H	15.0	−2.2	1.3	3.8
<hr/>				
—F	35.1	−14.3	0.9	−4.4
—Cl	6.4	0.2	1.0	−2.0
—Br	−5.4	3.3	2.2	−1.0
—I	−32.3	9.9	2.6	−0.4

( $\delta = 128.5$ ). The value of  $I$  depends on the nature of the substituent and its position relative to the C atom for which the shift is being calculated.

Several illustrative examples are given in Tab. 3.41. Larger deviations between calculated and observed values can be expected when the additivity of the substituent effects is disturbed by steric or electronic interactions.

**Tab. 3.41** Calculated and observed  $\delta$  values for the  $^{13}\text{C}$  shifts of substituted benzenes

Compound	C atom	$\delta_{\text{calculated}}$	$\delta_{\text{observed}}$
<i>p</i> -Xylene	C-1	134.7	134.5
	C-2	129.1	129.1
<hr/>			
Mesitylene	C-1	137.8	137.6
	C-2	126.6	127.4
<hr/>			
Hexamethylbenzene	C	135.9	132.3
<hr/>			
<i>p</i> -Cresol	C-1	152.3	152.6
	C-2	115.9	115.3
	C-3	130.7	130.2
	C-4	130.2	130.5
<hr/>			
3,5-Dimethoxybenzaldehyde	C-1	137.8	138.4
	C-2	106.1	107.0
	C-3	160.2	161.2
	C-4	103.9	107.0
<hr/>			
1-Chloro-2,4-dimethoxy-5-nitrobenzene	C-1	112.5	113.8
	C-2	166.9	159.9
	C-3	100.3	97.2
	C-4	153.4	154.5
	C-5	126.0	131.9
	C-6	125.2	127.7



## 4.8 Special Methods

Many of the methods already described for  $^1\text{H}$  NMR are also applicable to  $^{13}\text{C}$  NMR. These include the variation of the magnetic field strength and the solvent (see p. 124 and 126) and the measurement of temperature dependent spectra (see Sec. 2.2 and 2.3). In the following sections spin decoupling, the spin echo, spectral integration, the use of shift reagents, specific isotopic labelling, NOE experiments, polarisation transfer, double quantum transitions, two-dimensional  $^{13}\text{C}$  NMR spectroscopy, solid state spectroscopy (magic angle spinning), and the use of  $^{13}\text{C}$  databases will be described.

### Spin Decoupling: Heteronuclear Double Resonance

In  $^1\text{H}$  NMR coupled spectra are normally observed. Decoupling is only employed as a special experiment to aid signal assignment in difficult structural problems (see p. 131 ff.). Routine  $^{13}\text{C}$  NMR spectra are in contrast **proton broadband decoupled** (see Sec. 4.1, p. 142). This method of measurement is frequently referred to as  $^{13}\text{C}\{-^1\text{H}\}$  NMR (**proton noise decoupling**).

Because of the low natural abundance of  $^{13}\text{C}$  of 1.1%  $^{13}\text{C}$ ,  $^{13}\text{C}$  couplings are normally not observed. Couplings to  $^1\text{H}$ , D,  $^{19}\text{F}$ ,  $^{31}\text{P}$ , etc. however are observed. The **proton broadband decoupling** causes all couplings to protons to be removed, so that all the multiplets caused by  $^{13}\text{C}, ^1\text{H}$  coupling collapse to singlets. This simplifies the  $^{13}\text{C}$  spectra enormously. There is also a considerable gain in signal intensity, caused by the removal of the splittings and additionally by the **nuclear Overhauser effect** (see Sec. 4.1, p. 142 ff.).

To achieve proton broadband decoupling a high intensity of radiation must be applied to the sample to cover the whole of the proton frequency range. This is in fact a case of heteronuclear multiple resonance. If the decoupling power is too low, only the quaternary C atoms give sharp, intense signals, all other C atoms give relatively broad signals. This phenomenon can be used systematically to identify the quaternary C atoms (**low power noise decoupling**).

A serious disadvantage of proton broadband decoupling is the total loss of information about the multiplicity of the signals derived from direct  $^{13}\text{C}, ^1\text{H}$  couplings, i.e. the differentiation between primary ( $\text{CH}_3$ ), secondary ( $\text{CH}_2$ ), tertiary (CH), and quaternary (C) carbon atoms. This disadvantage can be overcome by **proton off-resonance decoupling**, the J-modulated spin-echo experiment described on p. 168, or the DEPT experiment described on p. 174. For off-resonance decoupling a decoupling frequency outside the shift range of the protons is chosen and no noise modulation is applied. This leads to a reduction of the coupling constants, so that in general only the direct  $^1J^{\text{R}}(\text{C},\text{H})$  couplings are visible. The magnitude of the reduced coupling constants  $^1J^{\text{R}}$  increases with the magnitude

of  $^1J$ , with the difference between the relevant  $^1\text{H}$  resonance frequency and the irradiation frequency, and with decreasing irradiation power; typical values of  $^1J^{\text{R}}$  are ca. 30–50 Hz. It is useful to vary the conditions as appropriate to produce the minimal overlap of the **quartet, triplet, doublet, and singlet signals** of the  $\text{CH}_3^*$ ,  $\text{CH}_2^*$ , CH groups, and quaternary C atoms.

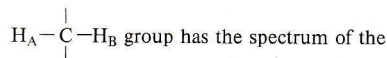
Since the nuclear Overhauser effect is still effective in the case of off-resonance decoupling, the measurement time required is less than for a fully coupled  $^{13}\text{C}$  NMR spectrum (but still longer than for a normal, broadband decoupled spectrum).

In Fig. 3.68 the proton broadband decoupled, off-resonance, and coupled spectra of ethylbenzene (**195**) are shown for comparison.

In the off-resonance spectrum the methyl signal a is split into a quartet, the methylene signal b into a triplet, and the signals of the protonated benzene C atoms c, d, and e into doublets. The quaternary C atom remains as a singlet. All the coupling constants are reduced. (Since the decoupler frequency was placed on the low field side, the reduction of the coupling constants is stronger on the low-field side of the spectrum than on the high-field side.)

In the coupled spectrum 3.68c the multiplets overlap. As a result, the aromatic part is very confusing. Figs. 3.68d and e show expansions of the aliphatic and aromatic parts of the spectrum respectively. More splittings than those due to  $^1J(\text{C},\text{H})$  couplings are apparent. The exact interpretation of coupled  $^{13}\text{C}$  spectra is often made difficult by two factors: firstly by the already mentioned overlap of multiplets (a particular problem in the case illustrated for the signals d and e) and secondly by the appearance of coupling patterns which do not obey the **rules for first order spectra**. This is clearest for C atom c. The left and right hand parts of this doublet are different. The asymmetry of such spin multiplets is a result of the mixing of nuclear spin states of similar energies. This phenomenon can even occur when the  $^1\text{H}$  NMR spectrum of the  $^{12}\text{C}$  **isotopomer** is first order.

\* This assumes the equivalence of geminal protons. An



X part of an ABX system, which is not always a 1 : 2 : 1 triplet.

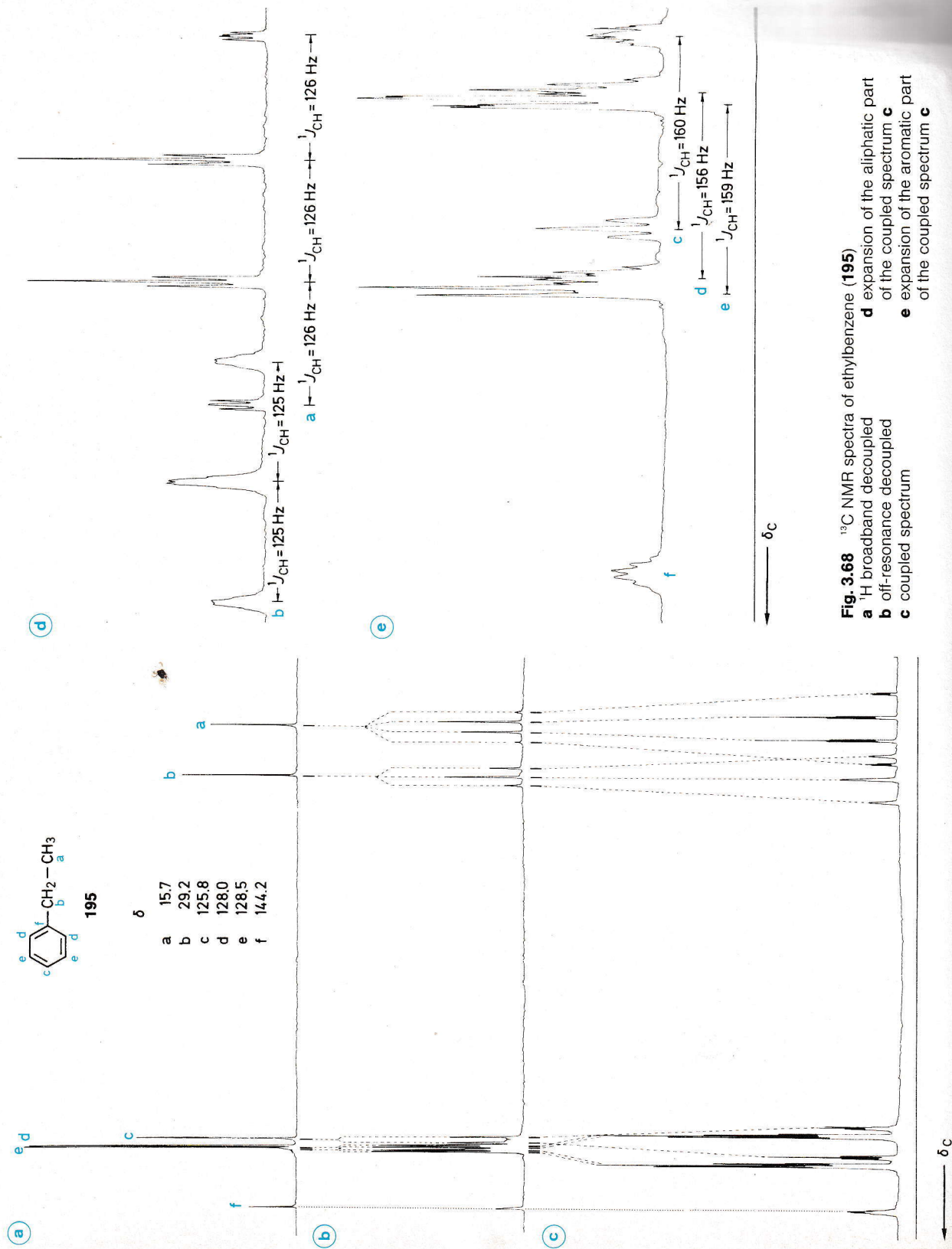


**Fig. 3.68**  $^{13}\text{C}$  NMR spectra of ethylbenzene (195)

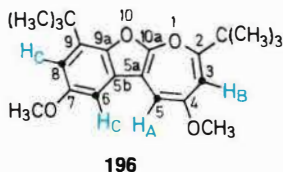
- a**  $^1\text{H}$  broadband decoupled
- b** off-resonance decoupled
- c** coupled spectrum
- d** expansion of the aliphatic part of the coupled spectrum **c**
- e** expansion of the aromatic part of the coupled spectrum **c**



A heteronuclear double resonance experiment can naturally also be carried out in such a way that the frequency of a single proton signal is irradiated. In the <sup>13</sup>C spectrum only the <sup>13</sup>C, <sup>1</sup>H couplings arising from this proton signal are removed. For the remaining <sup>13</sup>C signals the conditions are those of off-resonance decoupling, i.e. multiplets with reduced coupling constants are observed. This **selective decoupling (single frequency decoupling, SFD)** relies on the proton signals being reasonably well separated. (If necessary this may be achieved by employing a higher magnetic field strength or by the use of lanthanide shift reagents.)

As an aid to understanding the various possibilities a schematic representation of the different decoupling methods is given in Fig. 3.69.

A further example of the practical application of selective heteronuclear double resonance is shown in Fig. 3.70 for the heterocyclic compound **196**.



The <sup>1</sup>H NMR spectrum is shown in Fig. 3.70a. Whereas clearly separated signals are observed for the *t*-butyl groups, the methoxy groups, and the protons H<sub>A</sub> and H<sub>B</sub> of the oxepine ring, the signals of the benzene protons H<sub>C</sub> are coincidentally isochronous.

In the proton broadband decoupled <sup>13</sup>C spectrum (Fig. 3.70 b) 18 singlets are observed, as expected for the 18 types of chemically non-equivalent carbon atoms in the molecule (a-r). The interesting question is which <sup>13</sup>C signals correlate with the signals of H<sub>A</sub>, H<sub>B</sub>, and H<sub>C</sub>. This was determined by successively irradiating at the frequency  $\nu$  of the protons; the <sup>13</sup>C spectra obtained from these heteronuclear double resonance experiments are shown in Figs. 3.70 c, d, and e. On irradiating at the frequency of H<sub>A</sub> (Fig. 3.70c) C<sub>j</sub> appears as a singlet and C<sub>g</sub>, C<sub>i</sub>, and C<sub>k</sub> as doublets. This allows the first unambiguous assignment: H<sub>A</sub> is bonded to C<sub>j</sub>. From the magnitudes of the reduced couplings for C<sub>k</sub>, C<sub>i</sub>, and C<sub>g</sub> it can additionally be concluded, that H<sub>B</sub> belongs with C<sub>g</sub>. The final proof is provided by irradiating at  $\nu_B$  (Fig. 3.70d). For the protons H<sub>C</sub> the C atoms C<sub>i</sub> and C<sub>k</sub> are the only remaining possibilities. As a control experiment an irradiation was carried out at  $\nu_C$  (Fig. 3.70e). As expected, both the doublets of C<sub>i</sub> and C<sub>k</sub> collapse to singlets. The quaternary C-atoms can be assigned with the aid of increment systems and from comparisons with related systems. Overall this gives the following assignments:

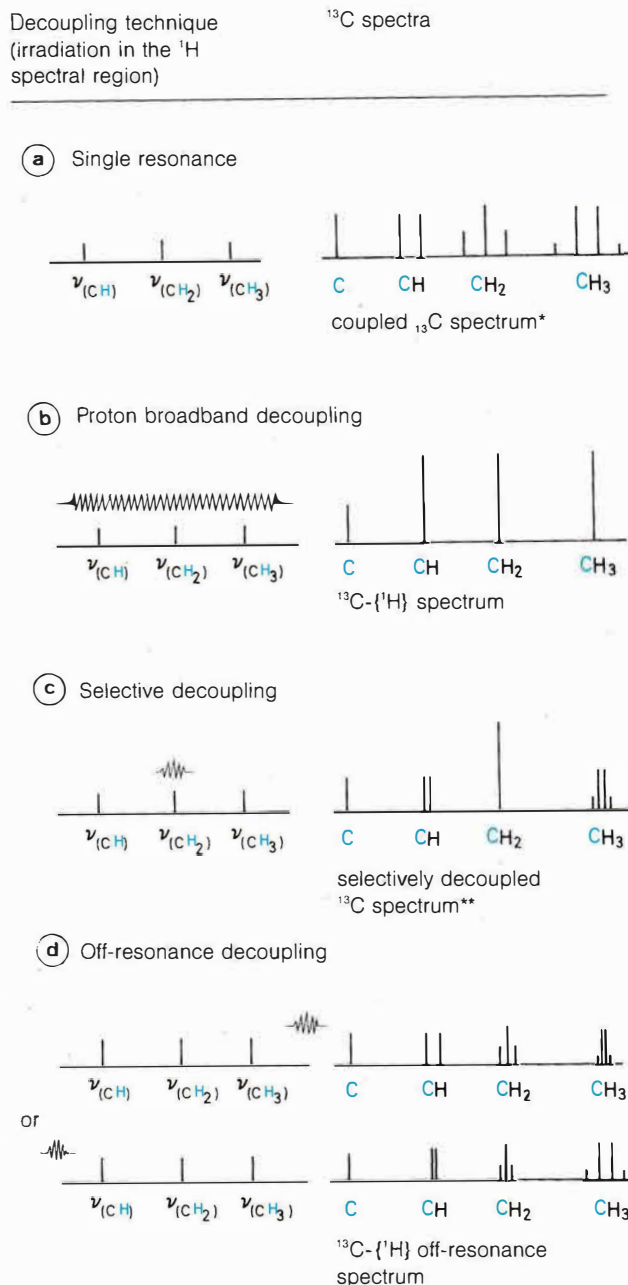


**Fig. 3.69** Schematic diagram showing the various decoupling techniques in the measurement of <sup>13</sup>C NMR spectra

\* Only direct <sup>13</sup>C, <sup>1</sup>H couplings are represented in the diagrams  
 \*\* Similar decoupling at the frequency  $\nu(\text{CH})$  collapses the doublet, at  $\nu(\text{CH}_2)$  the quartet



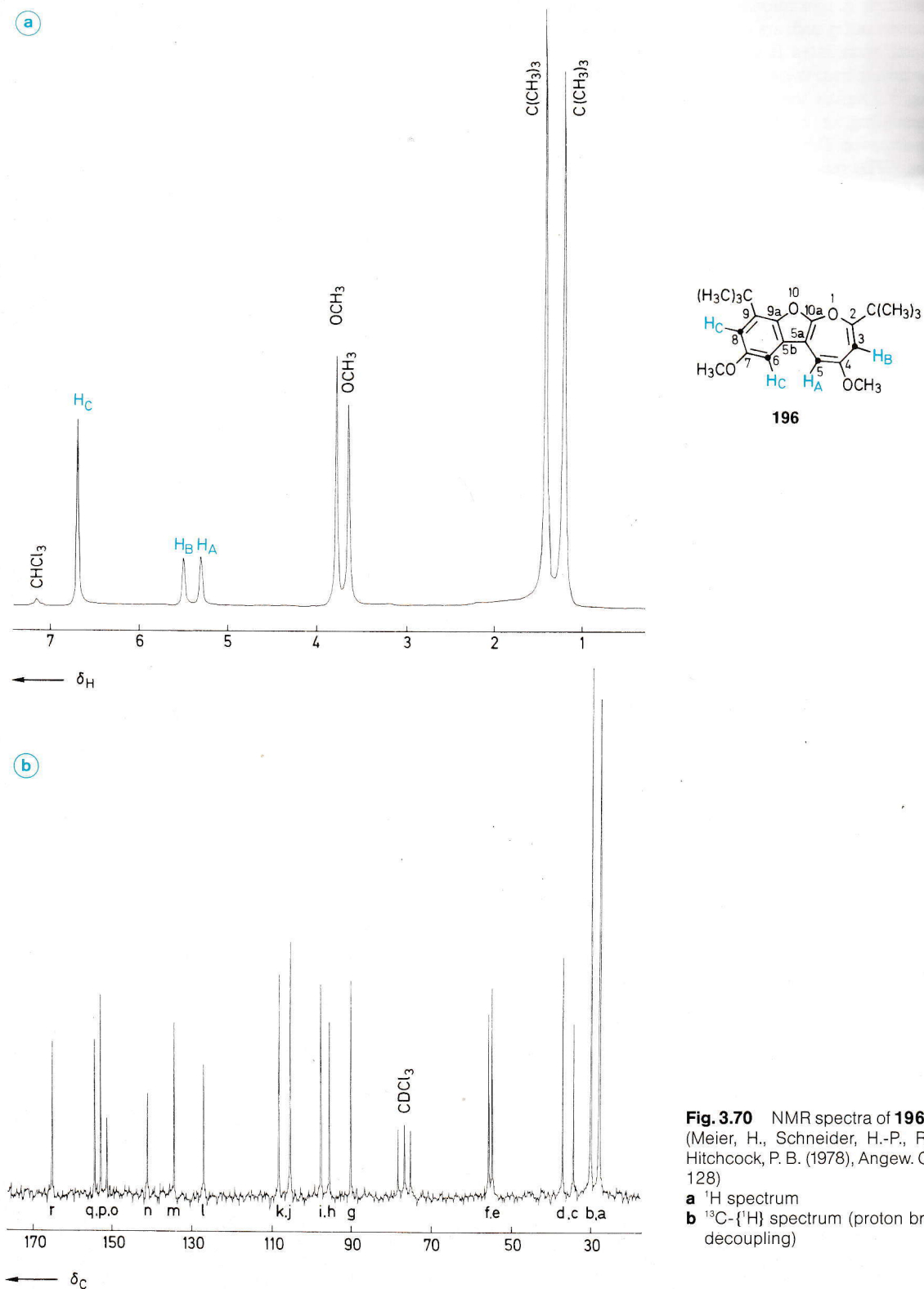


**Fig. 3.70** NMR spectra of **196** in  $\text{CDCl}_3$  (Meier, H., Schneider, H.-P., Rieker, A., Hitchcock, P. B. (1978), *Angew. Chem.* **90**, 128)

**a**  $^1\text{H}$  spectrum  
**b**  $^{13}\text{C}$ - $\{^1\text{H}\}$  spectrum (proton broadband decoupling)

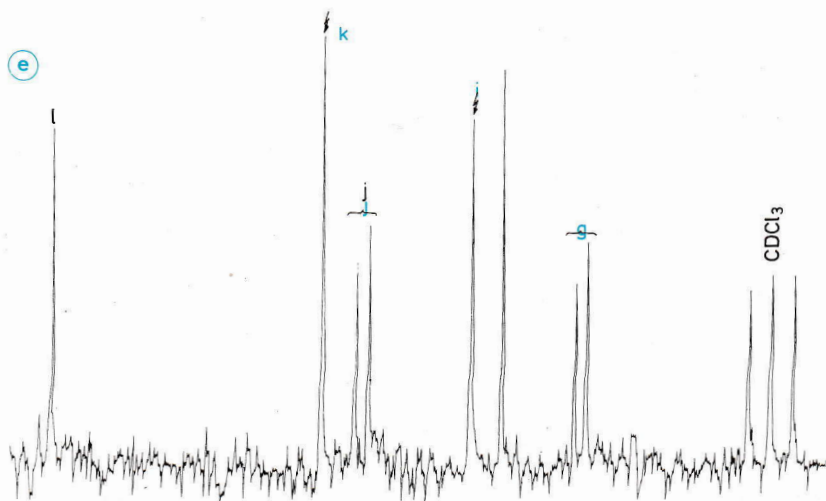
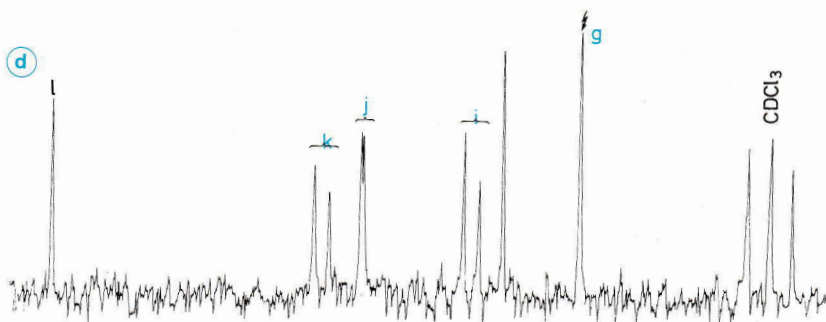
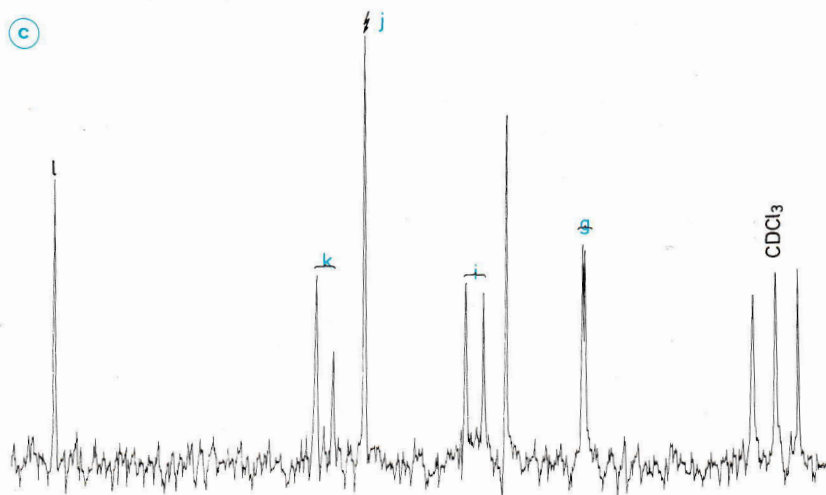


**Fig. 3.70** continued  
**c** Expansion of <sup>13</sup>C spectrum from double resonance experiment  $\nu_A$   
**d** Expansion of <sup>13</sup>C spectrum from double resonance experiment  $\nu_B$   
**e** Expansion of <sup>13</sup>C spectrum from double resonance experiment  $\nu_C$

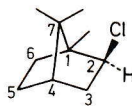
C-2: r:  $\delta = 166.7$   
 C-3: j:  $\delta = 106.0$   
 C-4/7: p, q:  $\delta = 154.5/156.0$

C-5: g:  $\delta = 90.6$   
 C-5a: h:  $\delta = 96.1$   
 C-5b: l:  $\delta = 128.0$   
 C-6: i:  $\delta = 98.3$   
 C-7/4: p, q:  $\delta = 154.5/156.0$

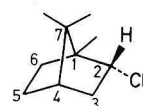
C-8: k:  $\delta = 108.9$   
 C-9: m:  $\delta = 135.6$   
 C-9a: n:  $\delta = 142.4$   
 C-10a: o:  $\delta = 152.9$

OCH<sub>3</sub> = e, f:  $\delta = 54.8/55.6$

C(CH<sub>3</sub>)<sub>3</sub> = a, b:  $\delta = 27.5/29.6$   
 = c, d:  $\delta = 34.1/36.9$



exo-2-Chloro-1,7,7-trimethylbicyclo[2.2.1]-heptane (isobornyl chloride, **197**)



endo-2-Chloro-1,7,7-trimethylbicyclo[2.2.1]-heptane (bornyl chloride, **198**)

Position	$\delta$	$\delta$
C-1	49.7	50.7
C-2	68.2	67.1
C-3	42.4	40.3
C-4	46.0	45.3
C-5	26.9	28.3
C-6	36.2	28.3
C-7	47.3	47.8
1-CH <sub>3</sub>	13.4	13.3
7-CH <sub>3</sub>	20.4/20.1	20.5/18.4

The quaternary C atoms C-1 and C-7 and the methylene groups H<sub>2</sub>C-3, H<sub>2</sub>C-5, and H<sub>2</sub>C-6 have positive signals when  $\tau = 1/J$ , the methine groups HC-2 and HC-4 and the methyl groups at C-1 and C-7 in contrast negative signals.

Fig. 3.71 shows the normal broadband decoupled <sup>13</sup>C spectrum of **197** and the *J*-modulated spin-echo spectrum.

### *J*-modulated Spin-echo

The *J*-modulated spin-echo experiment is an alternative to off-resonance decoupling (see p. 163) for the differentiation of the <sup>13</sup>C signals of CH<sub>3</sub>-, CH<sub>2</sub>-, CH-groups and quaternary carbons. This method has particular advantages for compounds which have closely spaced <sup>13</sup>C signals, where the off-resonance technique can lead to a confusing overlap of the partially decoupled multiplets. The method is based on the spin-echo pulse sequence: A 90° excitation pulse is followed after a time  $\tau$  by a 180° pulse, which inverts the transverse magnetisation. After a further time interval  $\tau$  the FID is observed. The <sup>1</sup>H decoupler is switched off during the second  $\tau$ -period, which causes a modulation of the signal intensity by the <sup>13</sup>C, <sup>1</sup>H coupling. The decoupler is switched back on immediately before the FID is accumulated, so the observed spectrum is decoupled, but the intensities of the signals of the CH<sub>*n*</sub>-groups depend on  $\tau$ , or more exactly on expressions containing the functions  $\cos(n\pi\tau/J)$ . If  $\tau = 1/J$  is chosen ( $\tau \approx 8$  ms for  $^1J(^{13}\text{C}, ^1\text{H}) = 125$  Hz), then positive signals are obtained for C- and CH<sub>2</sub>-groups ( $\cos 0$  and  $\cos 2\pi > 0$ ) and negative signals for CH- and CH<sub>3</sub>-groups ( $\cos \pi$  and  $\cos 3\pi < 0$ ). (An analogous experiment with  $\tau = 1/2J$  leads to a spectrum only showing the signals of quaternary carbons).

As an example the <sup>13</sup>C spectra of the bicyclic compounds **197** and **198** will be discussed.



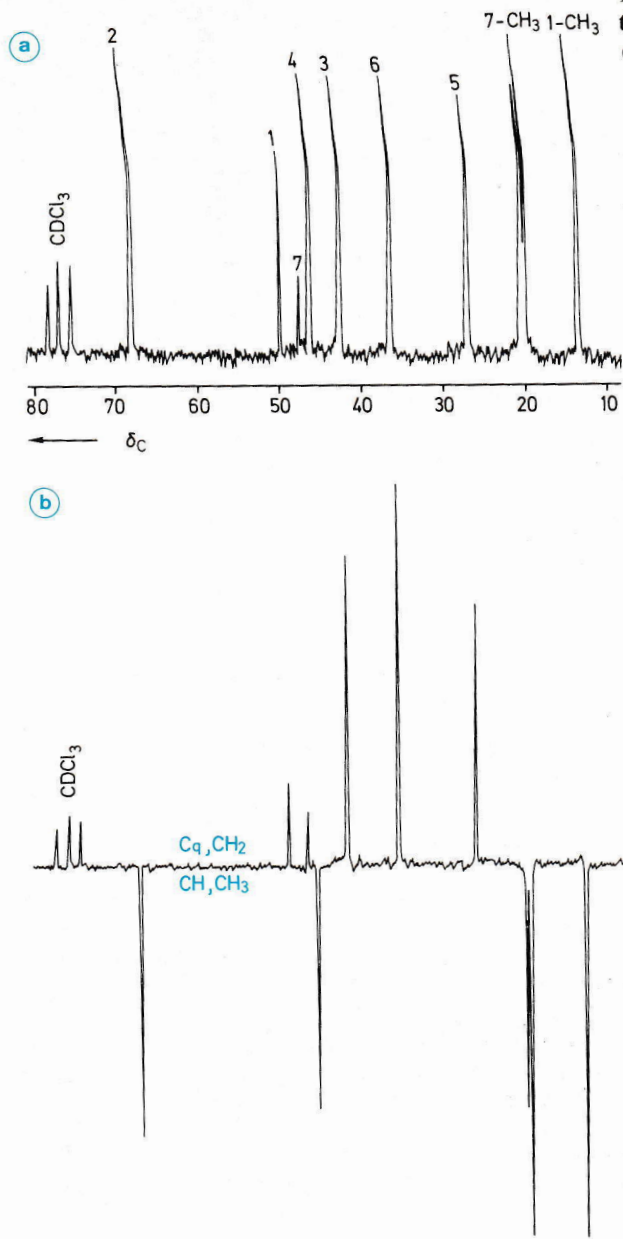


**Fig. 3.71** <sup>13</sup>C spectrum of isobornyl chloride (**197**) in CDCl<sub>3</sub>  
**a** <sup>1</sup>H broadband decoupling  
**b** J-modulated spin-echo spectrum ( $\tau = 1/J = 8$  ms)

**Spectrum Integration**

In contrast to <sup>1</sup>H spectra <sup>13</sup>C NMR spectra are not normally integrated (see Sec. 1.5, p. 84 f.).

This is because the signal intensities depend on the relaxation times of the various <sup>13</sup>C nuclei and in decoupled spectra on the different nuclear Overhauser effects.

Fig. 3.72 shows the marked influence of the measurement conditions. All four spectra were measured on the same solution of 4-ethyl-5-methyl-1,2,3-thiadiazole (**199**) using different values of the pulse length (PW). The other instrumental conditions remained unchanged (800 scans, 8K etc.). It can be seen that the relative intensity of the quaternary C atoms increases as the pulse length decreases. Decreasing the pulse length also worsens the signal/noise ratio considerably.

One possibility of obtaining spectra which yield useful integrations is the addition of paramagnetic relaxation reagents. Chromium and iron acetylacetonate have been found to be particularly useful (ca. 0.05 molar solution). Non-degassed samples contain dissolved oxygen, which also increases relaxation rates, particularly for the most slowly relaxing <sup>13</sup>C nuclei.

The magnetic moment of the unpaired electrons makes a new relaxation process effective, which dominates over other mechanisms. The different relaxation times of the different nuclei all become the same, and the nuclear Overhauser effect also becomes ineffective. The relaxation reagent must not react with the sample or even form weak complexes with it; otherwise the signals would be shifted as when paramagnetic shift reagents are used. Fig. 3.73 shows the integrated spectrum of 4-ethyl-5-methyl-1,2,3-thiadiazole (**199**) with added Cr(acac)<sub>3</sub>.

PW ( $\mu$ s)	Relative peak heights <i>h</i> and integrals <i>I</i>					
	C	a	b	c	d	e
12.0	<i>h</i>	44	100	67	18	9
	<i>I</i>	44	100	78	11	8
3.5	<i>h</i>	53	100	92	28	18
	<i>I</i>	53	100	97	21	18
1.0	<i>h</i>	66	100	83	69	39
	<i>I</i>	62	100	101	43	43
0.5	<i>h</i>	65	100	86	81	44
	<i>I</i>	57	100	120	52	48

The second method of obtaining useful integrations from <sup>13</sup>C spectra is the inverse gated decoupling method. (Normal gated decoupling is a method for measuring coupled spectra. The decoupler is only switched on during the period between the end of accumulation of one FID and the next pulse [pulse delay or relaxation delay]). This allows the nuclear Overhauser

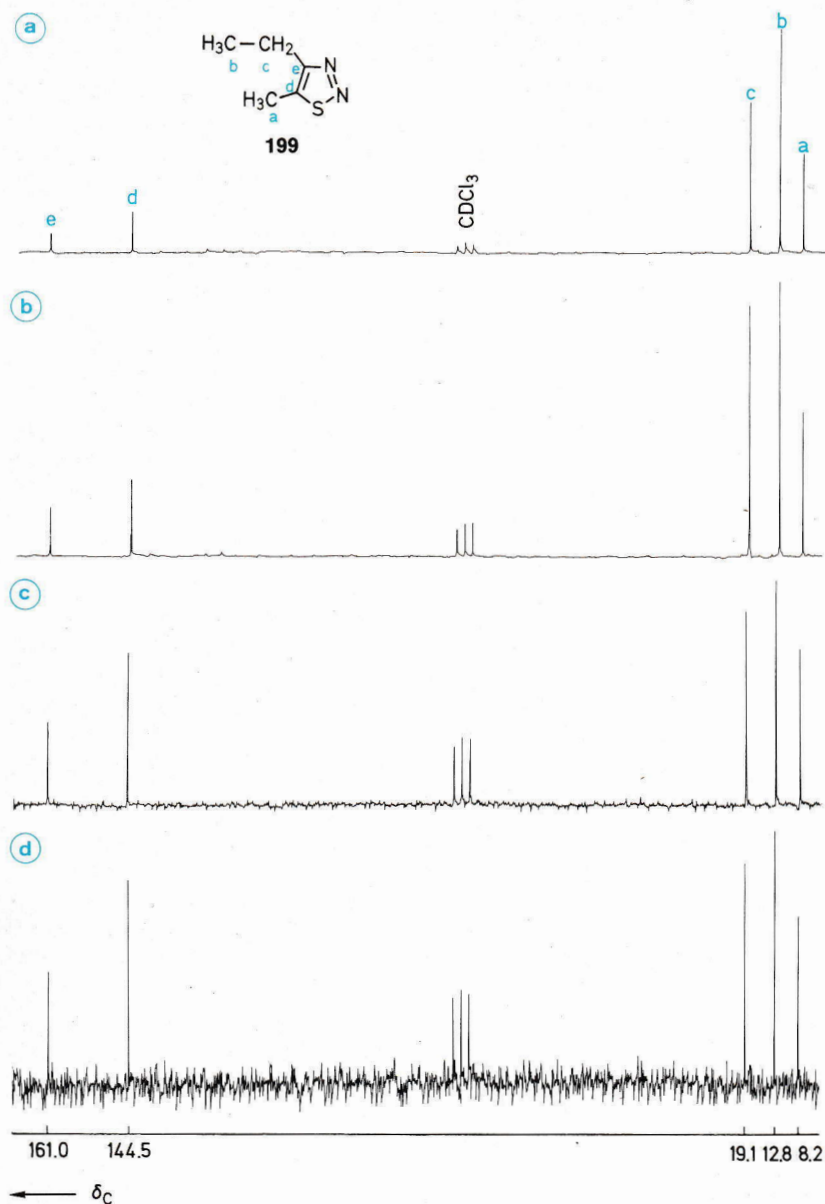


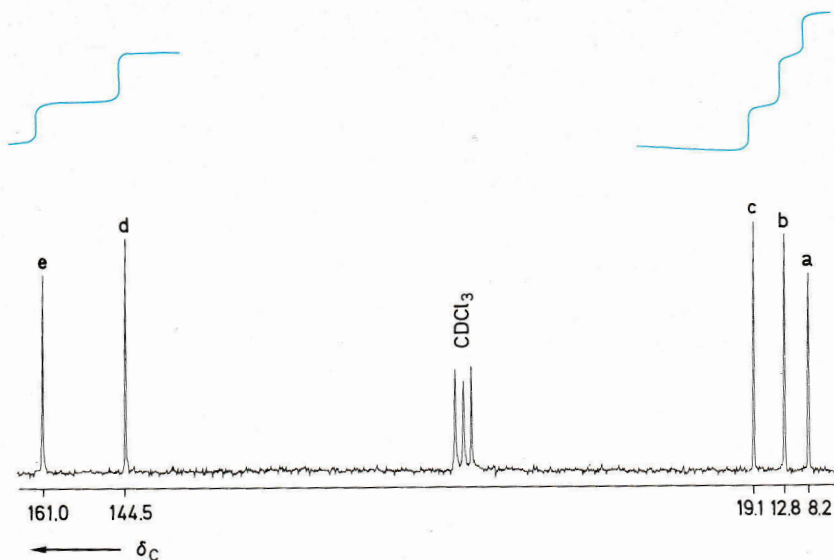
**Fig. 3.72**  $^1\text{H}$  broadband decoupled  $^{13}\text{C}$  spectrum of 4-ethyl-5-methyl-1,2,3-thiadiazole (**199**) in  $\text{CDCl}_3$  under identical measurement conditions apart from the pulse length; PW: 12  $\mu\text{s}$  (**a**), 3.5  $\mu\text{s}$  (**b**), 1.0  $\mu\text{s}$  (**c**), 0.5  $\mu\text{s}$  (**d**)

effect to enhance the intensity of signals of  $^{13}\text{C}$  nuclei with attached protons without decoupling the signals. Fully coupled  $^{13}\text{C}$  spectra are therefore best measured using this method of **gated proton decoupling**.) For inverse gated decoupling the decoupler is switched on during the accumulation of the FID (so that a decoupled spectrum is obtained) but switched off during the pulse delay. The latter needs to be long enough to allow complete relaxation of the nuclei and decay

of the nuclear Overhauser effect, which means that it must be longer than the longest  $^{13}\text{C}$   $T_1$  in the sample (occasionally  $T_1 \geq 100$  s!). Spin lattice relaxation and NOE then have no effect on the populations of the nuclear energy levels and therefore no effect on the signal intensities. The disadvantage of this method compared to the use of relaxation reagents is the long measurement times caused by the long pulse delays needed to ensure full relaxation.



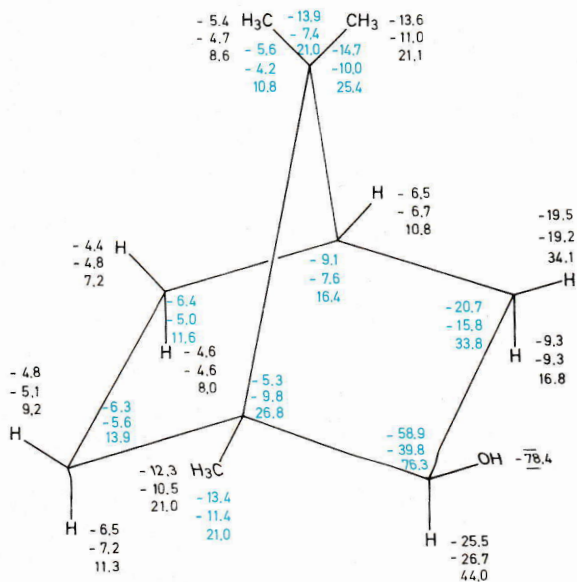
**Fig. 3.73** <sup>13</sup>C NMR spectrum (proton broadband decoupled) of 4-ethyl-5-methyl-1,2,3-thiadiazole (**199**) in CDCl<sub>3</sub> containing Cr(acac)<sub>3</sub> with integration curve



**Use of Lanthanide Shift Reagents**

An introduction to the use of **lanthanide shift reagents** in <sup>1</sup>H NMR was given on p. 128 ff. Essentially the same considerations apply to their use in <sup>13</sup>C spectroscopy. The total shift is made up of a **pseudo-contact** and a **contact term**. For chelate complexes of the lanthanides the (Fermi) contact term is generally small, and the **McConnell-Robertson equation** applies approximately (see p. 128). It therefore follows that <sup>1</sup>H

and <sup>13</sup>C nuclei in comparable positions (relative to the lanthanide central atom) should have the same shift. The literature values for isborneol (**200**) have been chosen as an example. The upper shift value refers to Eu(fod)<sub>3</sub>, the middle value to Eu(dpm)<sub>3</sub>, and the lower value to Pr(fod)<sub>3</sub>. The blue figures give the lanthanide-induced shifts for <sup>13</sup>C, the black figures the <sup>1</sup>H values. (Eu(fod)<sub>3</sub> and Eu(dpm)<sub>3</sub> shift to low field, Pr(fod)<sub>3</sub> to high field.)



**200**

**Specific Isotopic Labelling**

If one or more H atoms in a compound are substituted by **deuterium**, the <sup>13</sup>C spectrum changes in a very characteristic fashion.

Whereas CH, CH<sub>2</sub>, and CH<sub>3</sub> groups only show singlets in the <sup>1</sup>H broadband decoupled <sup>13</sup>C spectrum, a 1 : 1 : 1 triplet is observed for CD-, CHD-, and CH<sub>2</sub>D-groups, a 1 : 2 : 3 : 2 : 1 quintet for CD<sub>2</sub>- and CHD<sub>2</sub>-groups, and a 1 : 3 : 6 : 7 : 6 : 3 : 1 septet for CD<sub>3</sub>-groups (see p. 77).

The <sup>13</sup>C,D couplings are smaller than the corresponding <sup>13</sup>C,<sup>1</sup>H couplings by a factor γ<sub>H</sub>/γ<sub>D</sub> ≈ 6.5. <sup>13</sup>C,D long range couplings are therefore usually not observed. The H/D exchange is also noticeable by a small isotope effect on the <sup>13</sup>C shift: for <sup>13</sup>C-D a high-field shift of ca. 0.2 to 0.7 ppm is observed, for <sup>13</sup>C-C-D the isotope shift is even less (0.11 to 0.15 ppm).

More important is the fact that the nuclear Overhauser effect of fully deuteriated  $^{13}\text{C}$  nuclei (i.e. with no C-H bond) is reduced and the relaxation time is increased. These two factors combine to cause a considerable loss of signal intensity. Together with the splitting caused by  $^{13}\text{C},\text{D}$  coupling described above this often leads to the signals of fully deuteriated  $^{13}\text{C}$  nuclei disappearing partially or wholly into the noise. The signals of undeuteriated  $^{13}\text{C}$  nuclei are scarcely affected; at most they are split or broadened by the small  $^{13}\text{C},\text{D}$  coupling over two or three bonds.

H/D exchange is therefore a very valuable method for making unambiguous **signal assignments**. This goal can be approached even more directly with  $^{13}\text{C}$  labelling. The incorporation of  $^{13}\text{C}$

enriched carbon into specific positions in a molecule leads to intense  $^{13}\text{C}$  signals. With a small number of accumulations these may often be the only signals observed.  $^{13}\text{C}$  labelling also affords a convenient method of measuring  $^{13}\text{C},^{13}\text{C}$  coupling constants.

In Fig. 3.74 this is demonstrated using cyclopentanecarboxylic acid (**201**) as an example. Fig. 3.74a shows the  $^{13}\text{C}$  NMR spectrum of the normal, unlabelled material. In Fig. 3.74b, where C atom a has been enriched with  $^{13}\text{C}$  to a level of 50%, the signal of this carboxy C atom has greatly increased in intensity. The tertiary C atom b shows three peaks in the spectrum. The central line is the same as in Fig. 3.74a, being due to a  $^{13}\text{C}$  nucleus at b with only  $^{12}\text{C}$  neighbours. The two remaining lines are a

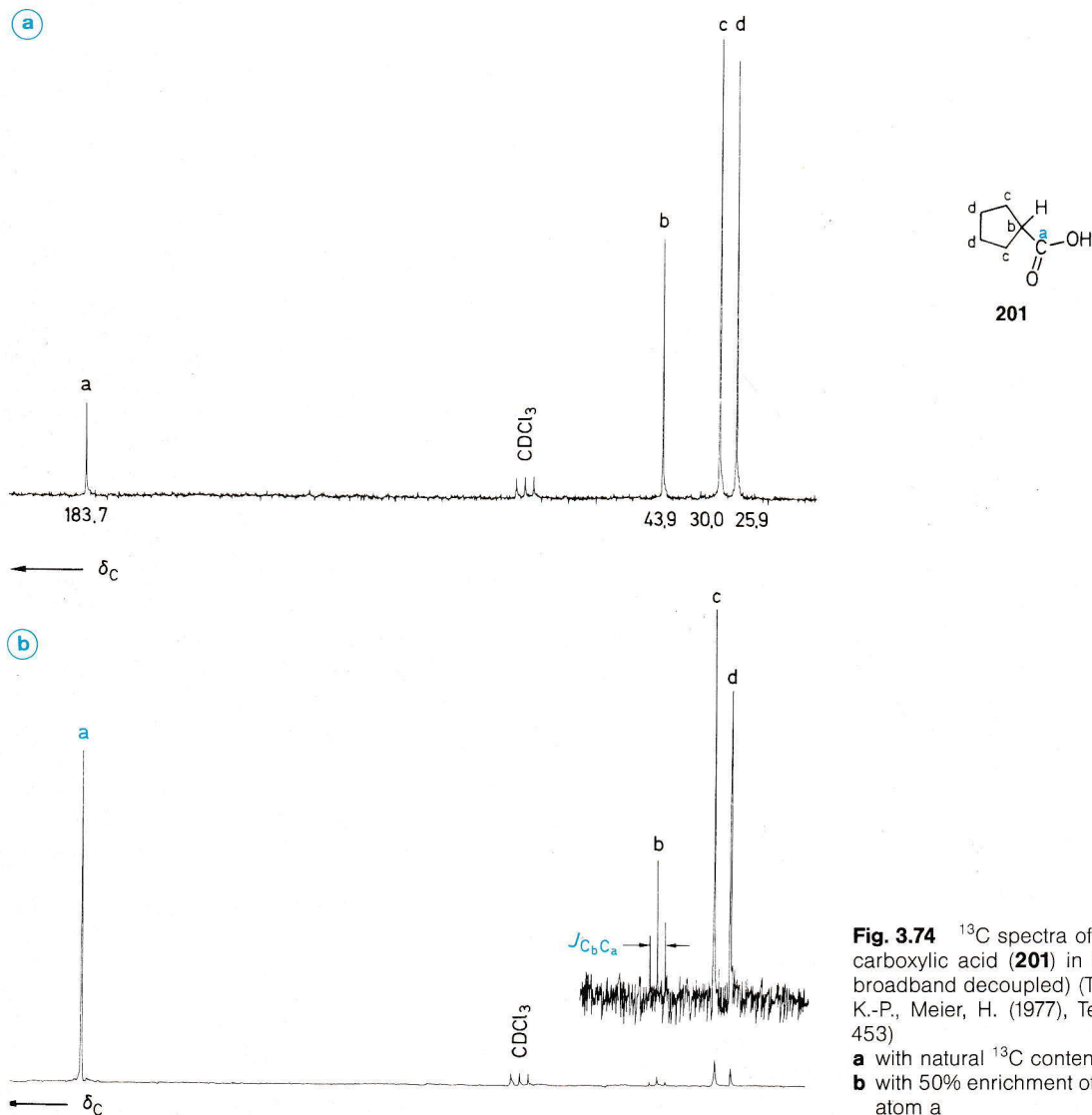


**Fig. 3.74**  $^{13}\text{C}$  spectra of cyclopentanecarboxylic acid (**201**) in  $\text{CDCl}_3$  (proton broadband decoupled) (Timm, U., Zeller, K.-P., Meier, H. (1977), *Tetrahedron* **33**, 453)

**a** with natural  $^{13}\text{C}$  content  
**b** with 50% enrichment of the carboxy C atom a



doublet, caused by <sup>13</sup>C nuclei at b with neighbouring <sup>13</sup>C nuclei at a. From the separation of the lines of this doublets the coupling constant  $^1J(C_b, C_a) = 56.8$  Hz can be obtained. (Because of the natural abundance of <sup>13</sup>C of 1.1% at nucleus b and the enrichment of nucleus b to a level of 50% every other <sup>13</sup>C nucleus at b has a <sup>13</sup>C neighbour at a, but only every ninety ninth nucleus a has a <sup>13</sup>C neighbour b).

Molecules (201)	a: <sup>12</sup> C; b: <sup>12</sup> C	a: <sup>13</sup> C; b: <sup>12</sup> C
<sup>13</sup> C signals	—;—	s;—
natural abundance	97.796%	1.096%
enrichment	49.45%	49.45%
Molecules (201)	a: <sup>12</sup> C; b: <sup>13</sup> C	a: <sup>13</sup> C; b: <sup>13</sup> C
<sup>13</sup> C signals	—; s	d; d
natural abundance	1.096%	0.012%
enrichment	0.55%	0.55%

The converse procedure, <sup>13</sup>C depletion below the natural abundance of 1.1%, is also of interest. The incorporation of <sup>13</sup>C depleted carbon leads to a disappearance of the relevant signals in the <sup>13</sup>C spectrum (For the use of <sup>12</sup>C enriched solvents see also p. 143).

Since a wide variety of D-, <sup>13</sup>C-, and <sup>12</sup>C-labelled compounds are commercially available, the synthesis of suitable labelled compounds is becoming an increasingly popular method for the unambiguous assignment of <sup>13</sup>C spectra. Such labelling techniques are of especial importance for following reaction pathways of organic and biochemical processes by NMR.

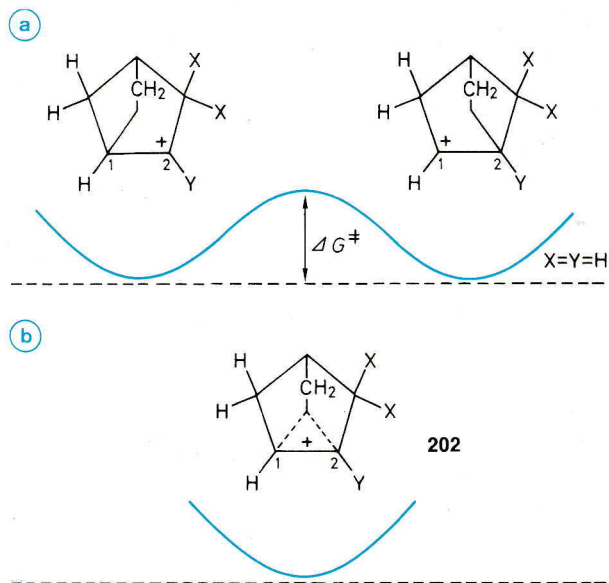
The isotopic perturbation method already described on p. 127 f. for <sup>1</sup>H NMR spectroscopy can naturally also be applied to <sup>13</sup>C NMR. The central problem of non-classical ions, the norbornyl cation (202) will be discussed as an example. There are two alternatives

- a) the double energy minimum model, with two “classical” ions in equilibrium
- b) the single energy minimum model of a symmetrical, non-classical ion.

After the incorporation of deuterium (X=D, Y=H/ X=H, Y=D) only a very small splitting of the <sup>13</sup>C signals of C-1 and C-2 is observed.

This is only compatible with the static model b. If there were a “perturbed equilibrium” of a fast Wagner-Meerwein rearrangement (Model a) the difference between the chemical shifts would be an order of magnitude larger.

Here borderline cases are naturally also feasible, involving a fast equilibrium between two species which only deviate very slightly from the symmetrical form.



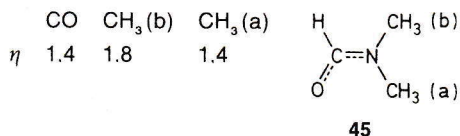
### NOE Measurements

In order to measure the <sup>13</sup>C,<sup>1</sup>H nuclear Overhauser effect (NOE) the signal intensities of <sup>1</sup>H decoupled and <sup>1</sup>H coupled spectra would normally need to be measured. The intensity determination is particularly inaccurate for coupled spectra. Therefore it is preferable in practice to compare the intensities of two decoupled spectra, one with, one without nuclear Overhauser effect. To produce the decoupled spectrum without Overhauser effect gated decoupling is used, with the decoupler only switched on during the pulse and the measurement of the FID. In the (long) pulse delay following accumulation of the FID the decoupler is switched off. This method relies on the fact that the nuclear Overhauser effect builds up relatively slowly, whereas the decoupling occurs almost spontaneously. If the <sup>13</sup>C relaxation only takes place through the dipole-dipole mechanism (i.e. as a result of the effect of the protons), the nuclear Overhauser effect is given by

$$\eta_C = \frac{\gamma_H}{2\gamma_C} = 1.988.$$

Much smaller values than this maximum are observed if other relaxation mechanisms are important.

The importance of NOE measurements in structure determination has already been indicated (see p. 134 ff.). An explicit example of the use of a heteronuclear NOE experiment is dimethylformamide (**45**) (Fig. 3.24, p. 94). At 25°C the following NOE factors are observed.

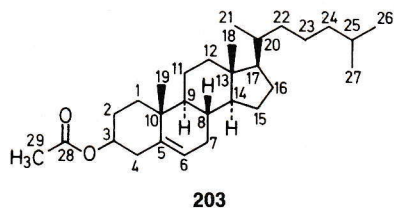


(a) is the CH<sub>3</sub>-group *anti* to the formyl hydrogen. Its signal lies at higher field and has a lower intensity than that of (b) in the broadband decoupled spectrum. With increasing temperature the exchange rate of the two methyl groups increases, and the difference between the two NOE factors decreases.

### Polarisation Transfer

From Tab. 3.1 (see p. 72) it can be seen that the natural abundance and the sensitivity of certain NMR measurable nuclei like <sup>13</sup>C and <sup>15</sup>N are very low. One reason for the low sensitivity is the low population difference between the two spin states (see Sec. 1.1, p. 71). Various methods are available (**SPI: selective population inversion, INEPT, DEPT pulse sequences**) which allow the transfer of the larger population difference for protons to a less sensitive nucleus (<sup>13</sup>C, <sup>15</sup>N, etc.) present in the same molecule. This **polarisation transfer** causes the transitions (absorption and emission!) to become stronger. The effect exceeds that due to the **nuclear Overhauser effect**.

One use of polarisation transfer is therefore to increase the signal intensity of <sup>1</sup>H decoupled or <sup>1</sup>H coupled <sup>13</sup>C spectra. A second application of **INEPT (insensitive nuclei enhanced by polarisation transfer)** or **DEPT (distortionless enhancement by polarisation transfer)** is the measurement of spectra in which peaks can be selected by their multiplicity (spectral editing). For example a <sup>1</sup>H decoupled or <sup>1</sup>H coupled <sup>13</sup>C spectrum of cholesteryl acetate (**203**) can be obtained in which only the CH<sub>2</sub>- or CH<sub>3</sub>-groups. **203** has a total of 29 chemically non-equivalent C atoms. The congestion of signals in the region between  $\delta = 20$  and  $\delta = 40$  is particularly high. In the normal decoupled or off-resonance decoupled spectra the signals are hopelessly overlapped.



CH <sub>3</sub>	$\delta$	CH <sub>2</sub>	$\delta$	CH	$\delta$	C <sub>q</sub>	$\delta$
C-18	12.0	C-1	37.3	C-3	73.7	C-5	139.9
C-19	19.3	C-2	28.2	C-6	122.6	C-10	36.7
C-21	18.9	C-4	38.4	C-8	32.2	C-13	42.5
C-26	22.7	C-7	32.2	C-9	50.4	C-28	169.6
C-27	22.9	C-11	21.3	C-14	57.0		
C-29	20.9	C-12	32.5	C-17	56.6		
		C-15	24.6	C-20	36.1		
		C-16	40.1	C-25	28.2		
		C-22	36.7				
		C-23	24.3				
		C-24	39.8				

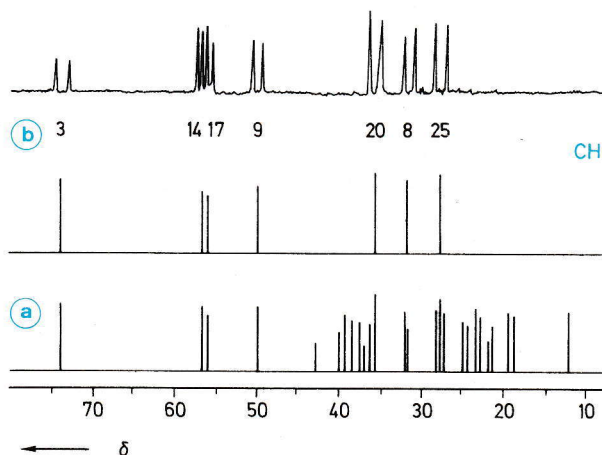


**Fig. 3.75** <sup>13</sup>C spectra of cholesteryl acetate (**203**) in CDCl<sub>3</sub>  
**a** Normal broadband decoupled spectrum of the saturated carbon atoms  
**b** Sub-spectrum of the methine groups (CH) coupled and decoupled (DEPT technique)

### Multidimensional <sup>13</sup>C NMR Spectra

As a complement to the section on p. 136 the applications of two-dimensional spectra to <sup>13</sup>C NMR will be briefly described.

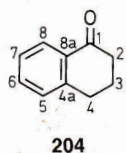


**J-resolved 2D <sup>13</sup>C spectra** give a separation of the parameters  $\delta(^{13}\text{C})$  and  $J(^{13}\text{C},^1\text{H})$ . Chemical shifts and  $^1J(\text{C},\text{H})$  coupling constants (multiplicities) can be instantly read off from the  $F_2$  and  $F_1$  axes respectively. Signal overlap, common in coupled <sup>13</sup>C spectra, which often causes difficulties with interpretation, is thereby avoided.

Using several examples more detail will be given about <sup>13</sup>C, <sup>1</sup>H shift correlation (**H,C COSY, HETCOR**).

In Fig. 3.76a the normal broadband decoupled <sup>13</sup>C spectrum of  $\alpha$ -tetralone (**204**) is shown. The signals of the quaternary C atoms are immediately recognisable by their low intensity. There remain the signals of the CH<sub>2</sub> groups H<sub>2</sub>C-2,3,4 and the CH groups HC-5,6,7,8.

The contour plots reproduced in Fig. 3.76 b and c allow an unambiguous assignment of the correspondence of the <sup>13</sup>C and <sup>1</sup>H signals. Thus it can be directly deduced that the <sup>13</sup>C nucleus with  $\delta = 126.7$  bears a proton that absorbs at  $\delta = 8.00$ , or that the carbon of the methylene group which absorbs at  $\delta = 2.85$  in the <sup>1</sup>H spectrum has  $\delta = 29.3$  etc. Finally, the individual proton signals are shown in Fig. 3.76 d. The doublet, triplet, or quintet structure, resulting from *vicinal* <sup>1</sup>H, <sup>1</sup>H couplings, is clearly visible without overlap. If the assignments of the <sup>1</sup>H spectrum are known, the shift correlation affords the <sup>13</sup>C assignments, and *vice versa*. If neither assignment is completely known, then the shift correlation, together with the splitting patterns and perhaps increment tables, is an especially valuable aid to the complete assignment of the <sup>13</sup>C and <sup>1</sup>H signals of a compound.

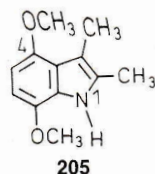


	$\delta(^{13}\text{C})$	$\delta(^1\text{H})$
C-1	197.7	-
C-2	38.8	2.55
C-3	22.9	2.04
C-4	29.3	2.85
C-4a	144.1	-
C-5	128.4	7.24
C-6	133.0	7.45
C-7	126.2	7.30
C-8	126.7	8.00
C-8a	132.2	-

able, which depend on the existence of smaller CH couplings ( $^2J_{\text{C,H}}$  and  $^3J_{\text{C,H}}$ ). 4,7-Dimethoxy-2,3-dimethylindole (**205**) will be discussed as an example.

Fig. 3.77 a shows the "normal" HETCOR spectrum (contour plot) with the correlations between directly bonded C and H atoms. This relies on the  $^1J_{\text{C,H}}$  couplings. The assignment of the six quaternary C atoms of **205** is possible by a long-range HETCOR measurement. The plot in Fig. 3.77 b shows the correlations arising from  $^3J_{\text{C,H}}$  and  $^2J_{\text{C,H}}$  couplings.

$^2J$	5-H—C-4
(--->)	6-H—C-5
	6-H—C-7
	3-CH <sub>3</sub> —C-3
	2-CH <sub>3</sub> —C-2
$^3J$	5-H—C-3a
(->)	5-H—C-7
	6-H—C-4
	6-H—C-7a
	3-CH <sub>3</sub> —C-3a
	3-CH <sub>3</sub> —C-2
	2-CH <sub>3</sub> —C-3
	4-OCH <sub>3</sub> —C-4
	7-OCH <sub>3</sub> —C-7



No correlation is visible for 5-H to C-6 ( $^2J_{\text{C,H}}$ ). The assignment of the individual quaternary C atoms is best done starting from a reliable reference point. C-7a for example can only show a single correlation,  $^3J$ , to 6-H.

In an analogy to the H-relayed (H,H) COSY experiment the magnetisation can be carried over from one proton, via another proton, to a <sup>13</sup>C nucleus. In Fig. 3.78 is shown part of an H-relayed (H,C) COSY spectrum of sucrose (**144**). By comparison with a normal <sup>13</sup>C, <sup>1</sup>H shift correlated 2D NMR spectrum the **relayed technique** employed, which correspond to <sup>13</sup>C nuclei and protons on neighbouring carbon atoms ( $^2J_{\text{C,H}}$ ):

To extend the technique to quaternary C atoms variants of the experiment (**long-range HETCOR, CH-COLOC**) are avail-

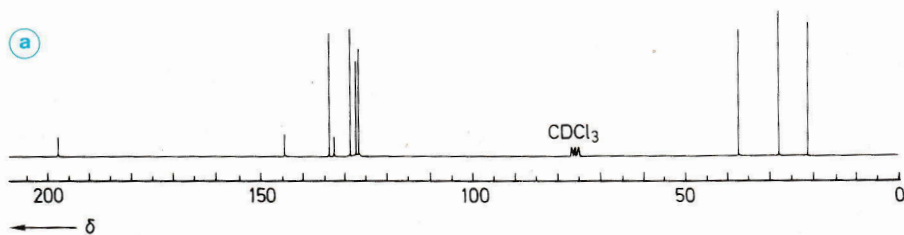


**Fig. 3.76** 2D NMR spectroscopy of  $\alpha$ -tetralone (**204**); (in CDCl<sub>3</sub>)  
a <sup>13</sup>C spectrum, broadband decoupled (1D spectrum)



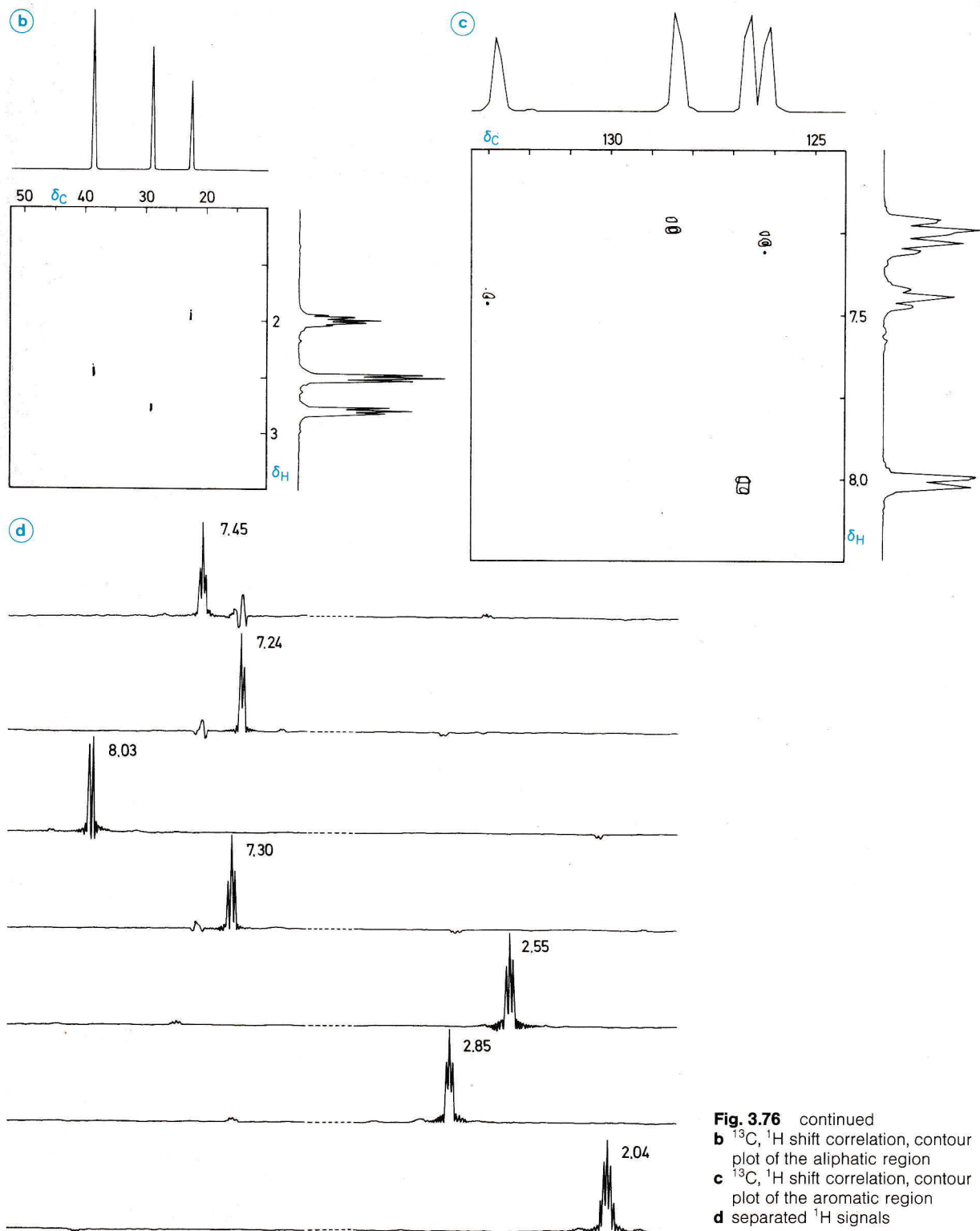


**Fig. 3.76** continued  
**b**  $^{13}\text{C}$ ,  $^1\text{H}$  shift correlation, contour plot of the aliphatic region  
**c**  $^{13}\text{C}$ ,  $^1\text{H}$  shift correlation, contour plot of the aromatic region  
**d** separated  $^1\text{H}$  signals

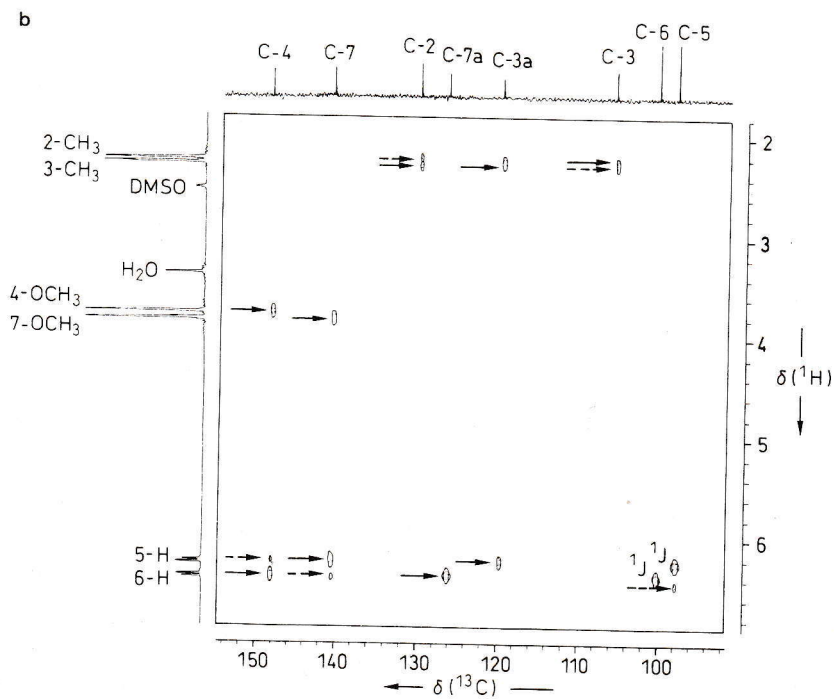
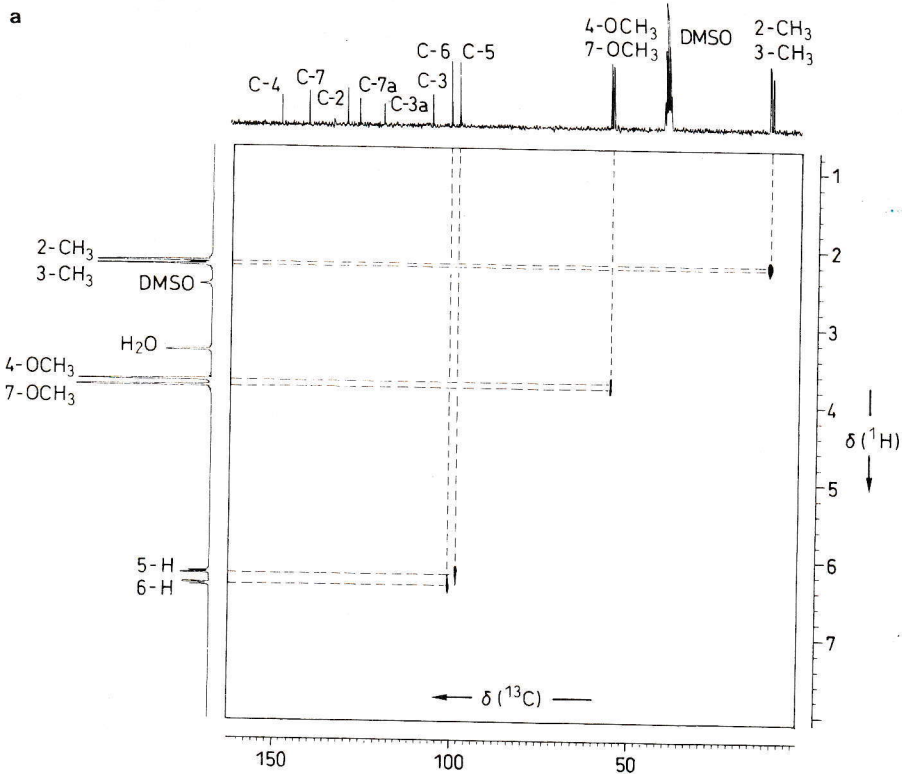


**Fig. 3.77** <sup>1</sup>H <sup>13</sup>C Heteronuclear shift correlation of 4,7-dimethoxy-2,3-dimethylindole (205) in DMSO-d<sub>6</sub>

**a** HETCOR  
**b** Long-range HETCOR

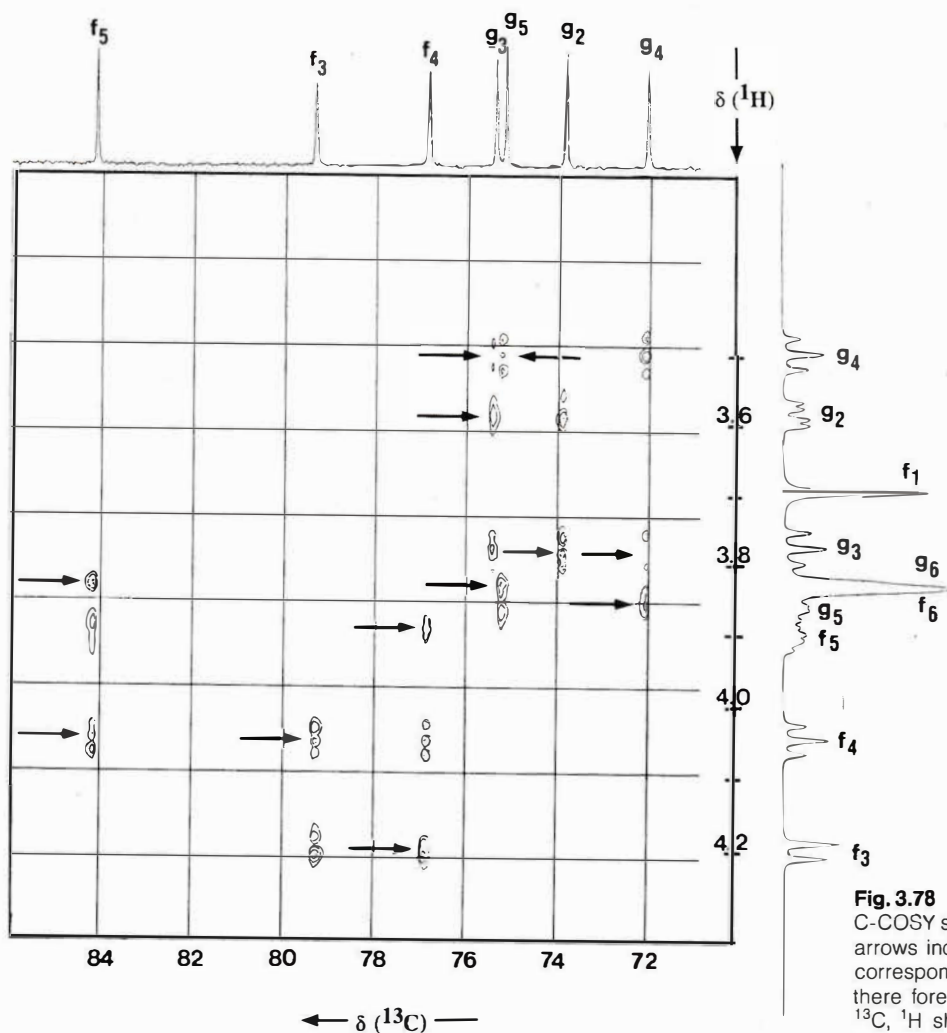


**Fig. 3.78** Expansion of an H-relayed H, C-COSY spectrum of sucrose (**144**) (The arrows indicate correlation peaks which correspond to  ${}^2J_{C, H}$  couplings, and there fore do not appear in the normal  ${}^{13}C$ ,  ${}^1H$  shift correlated 2D NMR spectrum)

Fructose ring	C-3/4-H ( $f_3 \rightarrow f_4$ )
	C-4/3-H and 5-H
	C-5/4-H and 6-H
	(C-1,2,6 not shown)
Glucose ring	C-2/3-H
	C-3/2-H and 4-H
	C-4/3-H and 5-H
	C-5/4-H and 6-H
	(C-1,6 and 1-H not shown)

For very complex structures a variety of three-dimensional techniques have been developed. For example it is of interest to combine the connectivity through bonds (2D) and the connectivity through space (2D) in a 3D measurement. A further application is the correlation of three different nuclear types. Fig. 3.79 shows a **three-dimensional  ${}^1H$ - ${}^{13}C$ - ${}^{15}N$  correlation spectrum** of  ${}^{13}C$  and  ${}^{15}N$  labelled ribonuclease T1, measured at 750 MHz. Each crosspeak indicates the  ${}^1H$  and  ${}^{15}N$  shift (cf. Sec. 6.3) of an N-H group in this higher protein. In the third dimension the connectivity to the  $\alpha$ -C atom of the next amino acid is indicated. The method allows a signal assignment related to the amino acid sequence.



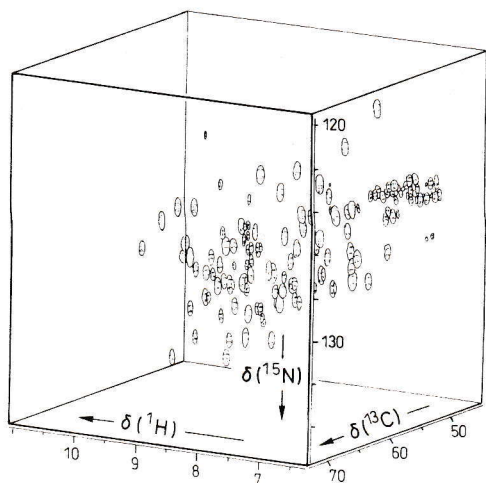
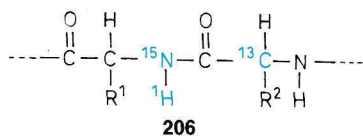
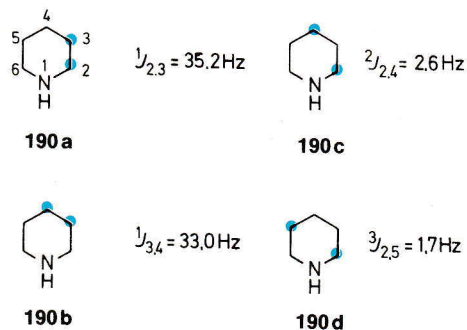


**Fig. 3.79** 750 MHz 3D <sup>1</sup>H-<sup>13</sup>C-<sup>15</sup>N-NH(CO)CA correlation spectrum of a 2 mM solution of <sup>13</sup>C and <sup>15</sup>N enriched ribonuclease T1 in H<sub>2</sub>O/D<sub>2</sub>O (Bruker, Analytische Messtechnik)

about 0.01% of the molecules contain **two** anisochronous <sup>13</sup>C nuclei and therefore fulfil the condition for the appearance of <sup>13</sup>C, <sup>13</sup>C coupling in the spectrum. The main signal arising from molecules with **one** <sup>13</sup>C nucleus is accompanied by low intensity satellites, which are however difficult to measure. This is particularly so when the coupling constants are small and the satellites lie under the wings of the main signal. The **INADEQUATE technique (incredible natural abundance double quantum transfer experiment)** suppresses the main signal. A special pulse sequence excites the **double quantum transitions**. A practical example, piperidine (**190**), is shown in Fig. 3.80. Four couplings are observed, arising from the isotopomers (**190a-d**) which are present in low concentration in normal piperidine.



Each AX (AB) spectrum is made up of four lines. In Fig. 3.80 the two components of each doublet appear in antiphase. The experimental conditions can be adjusted so that they appear as in phase doublets.

**Double Quantum Coherence for the Measurement of <sup>13</sup>C, <sup>13</sup>C Couplings**

As outlined in Sec. 4.5 (see p. 154), <sup>13</sup>C, <sup>13</sup>C couplings give valuable information about the C-C bonds present in a molecule. Because of the low natural abundance of <sup>13</sup>C (1.1%), only

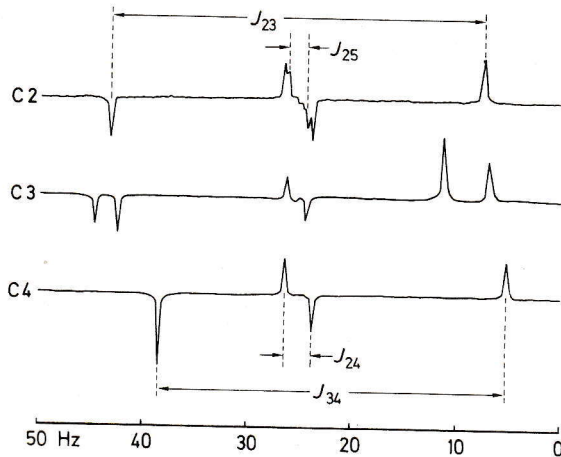


**Fig. 3.80** Sections of the <sup>13</sup>C NMR spectrum of piperidine (**190**): INADEQUATE experiment for the determination of the <sup>13</sup>C, <sup>13</sup>C coupling (Bax, A., Freeman, R., Kempell, S. T. (1980), J. Am. Chem. Soc. **102**, 4850)